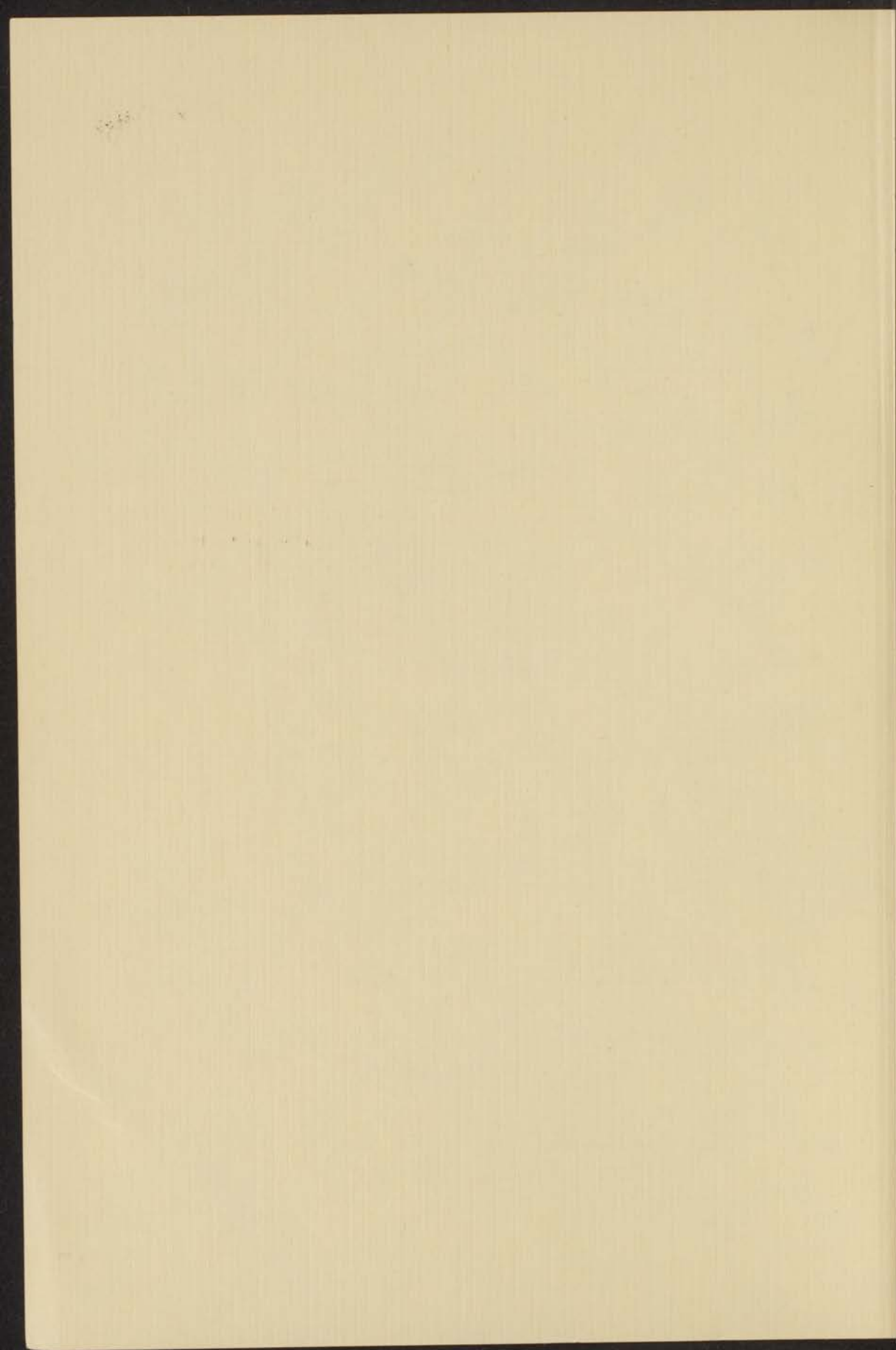


3 0 OKT. 1973

**THERMAL EFFECTS  
IN ADIABATIC FLOW OF He II**

**INSTITUUT-LOBENTZ**  
voor theoretische natuurkunde  
Nieuwsteeg 18-Leliden-Nederland

J. F. OLIJHOEK



30 OKT. 1973

THERMAL EFFECTS  
IN ADIABATIC FLOW OF He II

INSTITUUT-LOBENTZ  
voor theoretische natuurkunde  
Nieuwsteeg 18-Leyden-Nederland

kast dissertaties

THE THERMAL EFFECTS  
IN ADIABATIC FLOW OF H<sub>2</sub>

BY  
J. H. PERRY AND  
W. H. LINDSEY  
THE UNIVERSITY OF CALIFORNIA  
SAN DIEGO, CALIF.

Received March 10, 1954

# THERMAL EFFECTS IN ADIABATIC FLOW OF He II

PROEFSCHRIFT

TER VERKRIJGING VAN DE GRAAD VAN DOCTOR IN  
DE WISKUNDE EN NATUURWETENSCHAPPEN AAN DE  
RIJKSUNIVERSITEIT TE LEIDEN, OP GEZAG VAN DE  
RECTOR MAGNIFICUS DR. A.E. COHEN, HOOGLEERAAR  
IN DE FACULTEIT DER LETTEREN, VOLGENS  
BESLUIT VAN HET COLLEGE VAN DEKANEN TE  
VERDEDIGEN OP WOENSDAG 7 NOVEMBER 1973  
TE KLOKKE 14.15 UUR

door

JOHANNES FRANCISCUS OLIJHOEK  
geboren te 's-Gravenhage in 1942

THE THERMAL EFFECTS

PROMOTOR : PROF. DR. K.W. TACONIS  
CO-PROMOTOR: DR. R. DE BRUYN OUBOTER

DIT PROEFSCHRIFT IS BEWERKT MEDE ONDER TOEZICHT VAN  
DR. H. VAN BEELEN

## STELLINGEN

1. Uit een recent onderzoek van Berry volgt dat er geen discrepantie meer bestaat tussen de door El Hadi en Durieux in het interval van 2 tot 4 K gemeten waarden voor de dichtheid van de verzadigde damp van  $^4\text{He}$  en de met behulp van de toestandsvergelijking van het gas berekende waarden voor deze dichtheid.

*Berry, K.H., Thesis, University of Bristol (1972).*

*El Hadi, Z.E.H.A. and Durieux, M., Physica 41 (1969) 305.*

2. De tabel die Nishimura, Tinti en Vincent geven voor de vervalansen van de afzonderlijke spincomponenten van de fosforescerende triplettoestand van enkele diazanaftalenen is inconsistent in zichzelf.

*Nishimura, A.M., Tinti, D.S. and Vincent, J.S., Chem. Phys.*

*Letters 12 (1971) 360.*

3. Bij hun kritiek op de waarneming van zogenaamde Josephson stappen in de stroomkarakteristieken van He II zijn zowel Musinski en Douglass als Leiderer en Pobell stilzwijgend voorbijgegaan aan het feit dat de in die experimenten gemeten waarde van de grootte  $g\Delta Z_0/v$  binnen één procent overeenstemt met de waarde van  $h/m$ . Verder zou in een kritische beschouwing meer aandacht moeten worden besteed aan de kleine coherentielengte in helium wanneer men een vergelijking maakt met het corresponderende effect in supergeleiders.

*Richards, P.L. and Anderson, P.W., Phys. Rev. Lett. 14 (1965) 540.*

*Musinski, D.L. and Douglass, D.H., Phys. Rev. Lett. 29 (1972) 1541.*

*Leiderer, P. and Pobell, F., Phys. Rev. A7 (1973) 1130.*

*Khorana, B.M. and Douglass Jr., D.H., Proceedings of the Eleventh International Conference on Low Temperature Physics, University of St. Andrews Press, St. Andrews (1968) 169.*



4. Uit de interpretatie van de experimenten van Yu en Mercereau en van Clarke en de vergelijking tussen de hydrodynamica van He II en supergeleiders zoals gegeven door Putterman en De Bruyn Ouboter is duidelijk in te zien, dat de extra term die Khalatnikov in het geval van He II introduceert in de Landau-vergelijking van het superfluidum moet worden toegeschreven aan het niet in evenwicht zijn van de fracties van de twee fluida.

*Yu, M.L. and Mercereau, J.E., Phys. Rev. Lett. 28 (1972) 1117.*

*Clarke, J., Phys. Rev. Lett. 28 (1972) 1363.*

*Putterman, S. and De Bruyn Ouboter, R., Phys. Rev. Lett. 24 (1970) 50.*

*Khalatnikov, I.M., Introduction to the Theory of Superfluidity (W.A. Benjamin, Inc., New York, 1965).*

5. Aan de strenge vacuumeisen gesteld voor botsingsexperimenten met moleculaire bundels wordt niet zonder meer voldaan wanneer om veiligheidsredenen de gebruikelijke vloeibare waterstof in de cryopompen wordt vervangen door vloeibaar neon.

6. Ten onrechte hebben Rosenhein, Taube en Titus de coëfficiënt B die optreedt in de door hen voorgestane uitdrukking voor de frictiekracht op het superfluidum geïdentificeerd met de coëfficiënt B die Van Alphen c.s. hebben gevonden uit de experimenten aan de energiedissipatie in de stroming van superfluide helium.

*Rosenhein, J.S., Taube, J. and Titus, J.A., Phys. Rev. Lett. 26 (1971) 298.*

*Van Alphen, W.M., Olijhoek, J.F., De Bruyn Ouboter, R. and Taconis, K.W., Physica 32 (1966) 1901.*

7. Het verdient aanbeveling om bij experimenten zoals in dit proefschrift beschreven het drukverschil over het capillair te meten met behulp van capacitieve drukopnemers.

8. Het kan voordelen bieden het superlek dat uitmondt in de mengkamer van de Leidse alternatieve  $^3\text{He} - ^4\text{He}$  mengkoelmachine te vervangen door een capillair.

*Taconis, K.W., Pennings, N.H., Das, P. and De Bruyn Ouboter, R., Physica 56 (1971) 168.*



9. Door invoering van een cybernetisch model waarbij informatieverwerking en feedback de grondelementen zijn, ondergaat het ego van Freud hetzelfde lot als de Maxwell duivel: dit antropomorfe concept wordt overbodig.
10. Parijs rood lijkt een zeer geschikt materiaal voor de superlekken die gebruikt worden in experimenten met He II.

J.F. Olijhoek

Leiden, 7 november 1973

1. The first part of the paper is devoted to a general discussion of the problem of the stability of the equilibrium of a system of particles. It is shown that the stability of the equilibrium depends on the nature of the forces acting between the particles. In particular, it is shown that the equilibrium is stable if the forces are attractive and the particles are distributed in a regular lattice. On the other hand, the equilibrium is unstable if the forces are repulsive and the particles are distributed in a regular lattice.

2. In the second part of the paper, the stability of the equilibrium of a system of particles is studied in more detail. It is shown that the stability of the equilibrium depends on the nature of the forces acting between the particles and on the distribution of the particles. In particular, it is shown that the equilibrium is stable if the forces are attractive and the particles are distributed in a regular lattice. On the other hand, the equilibrium is unstable if the forces are repulsive and the particles are distributed in a regular lattice.

3. In the third part of the paper, the stability of the equilibrium of a system of particles is studied in more detail. It is shown that the stability of the equilibrium depends on the nature of the forces acting between the particles and on the distribution of the particles. In particular, it is shown that the equilibrium is stable if the forces are attractive and the particles are distributed in a regular lattice. On the other hand, the equilibrium is unstable if the forces are repulsive and the particles are distributed in a regular lattice.

4. In the fourth part of the paper, the stability of the equilibrium of a system of particles is studied in more detail. It is shown that the stability of the equilibrium depends on the nature of the forces acting between the particles and on the distribution of the particles. In particular, it is shown that the equilibrium is stable if the forces are attractive and the particles are distributed in a regular lattice. On the other hand, the equilibrium is unstable if the forces are repulsive and the particles are distributed in a regular lattice.

5. In the fifth part of the paper, the stability of the equilibrium of a system of particles is studied in more detail. It is shown that the stability of the equilibrium depends on the nature of the forces acting between the particles and on the distribution of the particles. In particular, it is shown that the equilibrium is stable if the forces are attractive and the particles are distributed in a regular lattice. On the other hand, the equilibrium is unstable if the forces are repulsive and the particles are distributed in a regular lattice.

6. In the sixth part of the paper, the stability of the equilibrium of a system of particles is studied in more detail. It is shown that the stability of the equilibrium depends on the nature of the forces acting between the particles and on the distribution of the particles. In particular, it is shown that the equilibrium is stable if the forces are attractive and the particles are distributed in a regular lattice. On the other hand, the equilibrium is unstable if the forces are repulsive and the particles are distributed in a regular lattice.

7. In the seventh part of the paper, the stability of the equilibrium of a system of particles is studied in more detail. It is shown that the stability of the equilibrium depends on the nature of the forces acting between the particles and on the distribution of the particles. In particular, it is shown that the equilibrium is stable if the forces are attractive and the particles are distributed in a regular lattice. On the other hand, the equilibrium is unstable if the forces are repulsive and the particles are distributed in a regular lattice.

INHOUD

1. Inleiding	1
2. De aard van de wet	2
3. De werking van de wet	3
4. De werking van de wet op de natuur	4
5. De werking van de wet op de mens	5
6. De werking van de wet op de maatschappij	6
7. De werking van de wet op de staat	7
8. De werking van de wet op de kerk	8
9. De werking van de wet op de familie	9
10. De werking van de wet op de school	10
11. De werking van de wet op de arbeid	11
12. De werking van de wet op de rust	12
13. De werking van de wet op de gezondheid	13
14. De werking van de wet op de veiligheid	14
15. De werking van de wet op de eer	15
16. De werking van de wet op de liefde	16
17. De werking van de wet op de vrede	17
18. De werking van de wet op de gerechtigheid	18
19. De werking van de wet op de wijsheid	19
20. De werking van de wet op de wijsheid	20
21. De werking van de wet op de wijsheid	21
22. De werking van de wet op de wijsheid	22
23. De werking van de wet op de wijsheid	23
24. De werking van de wet op de wijsheid	24
25. De werking van de wet op de wijsheid	25
26. De werking van de wet op de wijsheid	26
27. De werking van de wet op de wijsheid	27
28. De werking van de wet op de wijsheid	28
29. De werking van de wet op de wijsheid	29
30. De werking van de wet op de wijsheid	30

*Aan mijn ouders*

*Aan Harjolein en Harlies*

Deze afhandeling is geschreven door de schrijver van de afhandeling "De werking van de wet op de natuur". De afhandeling is geschreven in de stijl van de afhandeling "De werking van de wet op de mens". De afhandeling is geschreven in de stijl van de afhandeling "De werking van de wet op de maatschappij". De afhandeling is geschreven in de stijl van de afhandeling "De werking van de wet op de staat". De afhandeling is geschreven in de stijl van de afhandeling "De werking van de wet op de kerk". De afhandeling is geschreven in de stijl van de afhandeling "De werking van de wet op de familie". De afhandeling is geschreven in de stijl van de afhandeling "De werking van de wet op de school". De afhandeling is geschreven in de stijl van de afhandeling "De werking van de wet op de arbeid". De afhandeling is geschreven in de stijl van de afhandeling "De werking van de wet op de rust". De afhandeling is geschreven in de stijl van de afhandeling "De werking van de wet op de gezondheid". De afhandeling is geschreven in de stijl van de afhandeling "De werking van de wet op de veiligheid". De afhandeling is geschreven in de stijl van de afhandeling "De werking van de wet op de eer". De afhandeling is geschreven in de stijl van de afhandeling "De werking van de wet op de liefde". De afhandeling is geschreven in de stijl van de afhandeling "De werking van de wet op de vrede". De afhandeling is geschreven in de stijl van de afhandeling "De werking van de wet op de gerechtigheid". De afhandeling is geschreven in de stijl van de afhandeling "De werking van de wet op de wijsheid".

De afhandeling is geschreven door de schrijver van de afhandeling "De werking van de wet op de natuur".

Het in dit proefschrift beschreven werk is een onderdeel van het programma van de Stichting voor Fundamenteel Onderzoek der Materie (F.O.M.) en is mogelijk gemaakt door financiële steun van de Nederlandse Organisatie voor Zuiver Wetenschappelijk Onderzoek (Z.W.O.).

## CONTENTS

INTRODUCTION		9
CHAPTER I	The cooling effect in He II at saturated vapour pressure at various starting temperatures	11
1.	Introduction	11
2.	The apparatus	14
3.	Experimental results	17
3.1.	High-pressure head measurements	17
3.2.	Low-pressure head measurements	18
4.	Discussion	25
CHAPTER II	Measurements at high overall pressure; the mutual friction force and the influence of pressure on the limit for cooling	31
1.	Introduction	31
2.	Experimental set-up	33
3.	Experimental results	35
3.1.	Analysis of the results for $T_a > 1$ K	35
3.1.1.	The calculation of the mutual friction constant $A$ from the curves for which $\dot{Q}_H = 0$	38
3.1.2.	The calculation of $T_a$ as a function of $v$ for $\dot{Q}_H \neq 0$	42
3.1.2.a.	for $v = 0$	42
3.1.2.b.	for $T_a = 1.676$ K	45
3.2.	Measurements of $T_a$ close to its minimum value	48
CHAPTER III	The temperature distribution along the capillary during stationary flow of He II at saturated vapour pressure	59
1.	Introduction	59
2.	Experimental results	62
3.	Discussion and interpretation of the results	64
SAMENVATTING		78
STUDIEOVERZICHT		80

CONTENTS

	INTRODUCTION	
	CHAPTER I	
	The cooling effect in air at constant	
10	specific pressure at various starting temperatures	
11	Discussion	
12	The constants	
13	Experimental results	
14	Discussion of the results	
15	Experimental data	
16	Discussion of the data	
17	Discussion	
	CHAPTER II	
	Measurements of the cooling effect of air at constant	
	specific pressure and the influence of pressure on the	
	rate of cooling	
18	Discussion	
19	Experimental data	
20	Experimental results	
21	Discussion of the results for $T_1 = 20^\circ C$	
22	The variation of the cooling effect with constant $T_1$	
23	Discussion of the results for $T_1 = 20^\circ C$	
24	The variation of $T_1$ as a function of $T_2$	
25	Discussion	
26	Experimental data	
27	Experimental results	
28	Discussion of the results	
29	Discussion	
	CHAPTER III	
	The influence of the initial temperature on the	
	rate of cooling at constant specific pressure	
30	Discussion	
31	Experimental data	
32	Experimental results	
33	Discussion of the results	
34	Discussion	
35	Experimental data	
36	Experimental results	
37	Discussion of the results	
38	Discussion	
39	Experimental data	
40	Experimental results	
41	Discussion of the results	
42	Discussion	
43	Experimental data	
44	Experimental results	
45	Discussion of the results	
46	Discussion	
47	Experimental data	
48	Experimental results	
49	Discussion of the results	
50	Discussion	
51	Experimental data	
52	Experimental results	
53	Discussion of the results	
54	Discussion	
55	Experimental data	
56	Experimental results	
57	Discussion of the results	
58	Discussion	
59	Experimental data	
60	Experimental results	
61	Discussion of the results	
62	Discussion	
63	Experimental data	
64	Experimental results	
65	Discussion of the results	
66	Discussion	
67	Experimental data	
68	Experimental results	
69	Discussion of the results	
70	Discussion	
71	Experimental data	
72	Experimental results	
73	Discussion of the results	
74	Discussion	
75	Experimental data	
76	Experimental results	
77	Discussion of the results	
78	Discussion	
79	Experimental data	
80	Experimental results	
81	Discussion of the results	
82	Discussion	
83	Experimental data	
84	Experimental results	
85	Discussion of the results	
86	Discussion	
87	Experimental data	
88	Experimental results	
89	Discussion of the results	
90	Discussion	
91	Experimental data	
92	Experimental results	
93	Discussion of the results	
94	Discussion	
95	Experimental data	
96	Experimental results	
97	Discussion of the results	
98	Discussion	
99	Experimental data	
100	Experimental results	
101	Discussion of the results	
102	Discussion	
103	Experimental data	
104	Experimental results	
105	Discussion of the results	
106	Discussion	
107	Experimental data	
108	Experimental results	
109	Discussion of the results	
110	Discussion	
111	Experimental data	
112	Experimental results	
113	Discussion of the results	
114	Discussion	
115	Experimental data	
116	Experimental results	
117	Discussion of the results	
118	Discussion	
119	Experimental data	
120	Experimental results	
121	Discussion of the results	
122	Discussion	
123	Experimental data	
124	Experimental results	
125	Discussion of the results	
126	Discussion	
127	Experimental data	
128	Experimental results	
129	Discussion of the results	
130	Discussion	
131	Experimental data	
132	Experimental results	
133	Discussion of the results	
134	Discussion	
135	Experimental data	
136	Experimental results	
137	Discussion of the results	
138	Discussion	
139	Experimental data	
140	Experimental results	
141	Discussion of the results	
142	Discussion	
143	Experimental data	
144	Experimental results	
145	Discussion of the results	
146	Discussion	
147	Experimental data	
148	Experimental results	
149	Discussion of the results	
150	Discussion	

## INTRODUCTION

In the context of the two-fluid model for liquid He II, i.e. for liquid helium below a temperature of 2.172 K, the liquid may be regarded as if it were a mixture of two components, a superfluid component with density  $\rho_s$  and a normal component with density  $\rho_n$ . The superfluid carries no entropy and has no viscosity whereas the normal component carries all the entropy of the liquid and behaves as an ordinary viscous liquid. In this model the macroscopic flow of He II is described in terms of a motion of the superfluid with velocity  $v_s$  and of the normal fluid with velocity  $v_n$ .

The ability of the superfluid component to flow without friction through narrow channels, while the normal component is blocked by its viscosity makes it possible to separate both components. Therefore a so-called superleak which actually consists of a tube packed tightly with fine powders, when inserted in a circuit through which He II is flowing acts as an entropy filter. As was mentioned already by Kapitza, the method of forcing liquid He II through a superleak offers the possibility to create very low temperatures at the downstream side of the superleak. In this thesis a series of experiments performed to investigate the properties of a continuous cooling method based on this principle is described. In the apparatus used He II is forced to flow through a circuit consisting of a superleak and capillary in series connected to each other via a small chamber.

As will be shown cooling in the chamber occurs due to the fact that normal fluid is drained away through the capillary by means of the mutual friction between superfluid and normal fluid, and is replenished by pure superfluid coming through the superleak. It appears that in practice a limit for cooling of about 0.75 K occurs, which temperature is much higher than anticipated by Kapitza who a priori saw no reason for such a limit to occur.

A major part of the present work is therefore devoted to the question, why and how such a limit does occur. These questions run like a thread through all three chapters of this thesis. The results will be presented in the following way.

In Chapter I the experiments performed to investigate the influence of the starting temperature are reported.

Chapter II contains the experiments performed with helium under high



overall pressure. In these experiments the influence of pressure on the limit for cooling and the nature of the mutual friction force was studied.

The measurements of the temperature distribution along the capillary during stationary flow through the flow circuit which are presented in Chapter III help to give an answer to some questions which did arise in the two preceding chapters.

The first chapter and an abridged form of the second chapter have been published as separate papers in Physica.

The complete second chapter as well as the third chapter will be published separately shortly.

## CHAPTER I

### THE COOLING EFFECT IN He II AT SATURATED VAPOUR PRESSURE AT VARIOUS STARTING TEMPERATURES

#### *Synopsis*

Measurements on the cooling effect which occurs when liquid He II is forced to flow through a system consisting of a superleak and a fine capillary in series are reported. The nature of this cooling process and the origin of a lower limit which occurs at about 0.75 K, independently of the initial conditions, are the subjects of the present research. In carrying out the experiments at temperatures below 0.75 K, no cooling was detected; instead a warming occurred from which we were able to calculate the dissipative energy rate. It is found that the "mutual friction" force plays an essential role in the cooling process and that cooling is most likely due to interaction between rotons and vortices.

#### 1. *Introduction*

When liquid helium at a temperature lower than 2.172 K (superfluid or He II) is forced to pass through an ideal superleak, the liquid gives up its entropy <sup>1)</sup>. In the context of the two-fluid model of He II one would say that only the superfluid fraction (carrying no entropy and having no viscosity) has passed through the superleak, while the viscous normal fraction has been filtered out. The helium leaving the superleak possesses no entropy and would be at temperature zero <sup>2)</sup>. Kapitza anticipated that the method of forcing helium through a superleak into a vessel, empty or partially filled with He II would "a priori permit us to approach as close to absolute zero as our technical means will permit" <sup>3)</sup>.

The lowest temperature attainable in this way is limited by the normal excitations already present in the helium in the vessel. If there were a way to get rid of these excitations (or so-called normal fluid) while at the same time replenishing them by pure superfluid coming through the superleak, one could hope to obtain very low temperatures. Cooling by such a process, i.e.,

by convective heat transport, has been achieved in the apparatus sketched in fig. 1.

A superleak is followed in series by a chamber and a narrow capillary. Helium II passing through this system under a driving force supplied by a positive pressure difference  $\Delta P = \rho g \Delta Z$  will be forced to flow at supercritical velocities through the capillary. This implies that there will be a difference in the chemical potential over the capillary. The temperature at the beginning of the capillary,  $T_a$ , is seen to cool with respect to the downstream side of the capillary. As the velocity is increased (by increasing  $\Delta Z$ ),  $T_a$  is seen to decrease further, reaching a lower limit of about 0.75 K, regardless of the initial temperature of the helium above the superleak.

The first experiments on this continuous cooling method have been reported previously by some of the present authors<sup>4)</sup>. Staas and Severijns have carried out similar experiments with their so-called vortex cooler<sup>5)</sup>. They have explained the decrease of temperature in the following way.

In the arrangement depicted in fig. 1 the total difference in the chemical potential,  $\Delta\mu = g\Delta Z$ , occurs over the capillary (for a superleak  $\Delta\mu = 0$ , provided

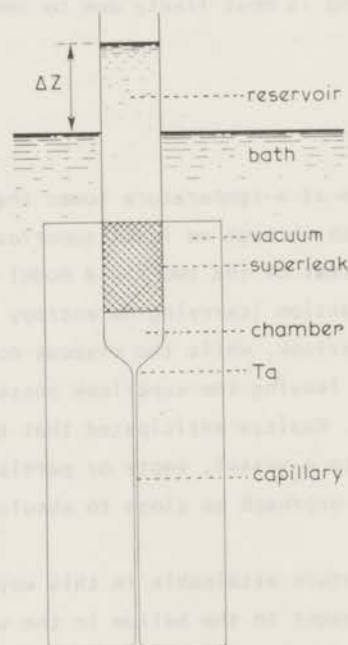


Fig. 1. Basic diagram of the cooling device.

that the critical velocity in the superleak is not surpassed). Making use of the thermodynamical identity

$$\Delta\mu = - \int_T^{T+\Delta T} s dT + \frac{1}{\rho} \Delta P \quad (1)$$

and the fact that initially there is no temperature difference over the capillary, one sees that  $\Delta\mu$  manifests itself as a pressure difference over the capillary. This pressure difference will drive the normal excitations out of the capillary. Hence a temperature difference is established over the capillary and, consequently, an opposing temperature difference must exist over the superleak. This gives rise to a fountain pressure difference over the superleak, in accordance with eq. (1), since  $\Delta\mu_{\text{superleak}} = 0$ . Therefore the pressure difference over the capillary will decrease as a result of the cooling process. A stationary situation will be reached when no more excitations are removed from the chamber, and it is suggested by Staas and Severijns<sup>5)</sup> that this situation will be reached when  $\Delta P_{\text{capillary}} = 0$ , so that the total difference in the chemical potential manifests itself as a temperature difference over the capillary.

From this simple explanation it follows immediately that if the applied difference in chemical potential is high enough, i.e., when it is equal to

$$- \int_{T=0}^{T=T_{\text{bath}}} s dT,$$

a temperature at  $T_a$  very close to zero will be reached. Even in the case that the pressure difference over the capillary does not disappear completely in the cooling process, very low temperatures should be attainable by applying a  $\Delta\mu$  higher than

$$\int_{T=0}^{T=T_{\text{bath}}} s dT.$$

However, the lowest temperatures attained experimentally are all close to a value of 0.75 K. Staas and Severijns<sup>5)</sup> have argued that this limit may be due to the heat leak through the superleak, this of course not being an ideal superleak. However, the construction of our apparatus was such that we were able to eliminate the heat leak through the superleak. The results of the experiments show clearly that the imperfection of the superleak is not responsible



for the limiting temperature of 0.75 K. In addition the apparatus enabled us to perform the experiments at starting temperatures ranging from 0.3 K to  $T_\lambda$ . From the explanation of the cooling principle given above one should expect cooling to occur for all starting temperatures (measurements by Bots and Gorter<sup>6)</sup> have shown that  $\Delta\mu$  over the superleak remains zero down to at least 0.1 K). However, in our experiments at a starting temperature of 0.5 K we observed that an *increase* in temperature at  $T_a$  occurred.

From both the above results we are led to the conclusion that the limiting temperature of about 0.75 K is an intrinsic property of the cooling process itself.

## 2. The apparatus

The apparatus, which is shown schematically in fig. 2, was designed to function at "full capacity" at 0.5 K. It consists of three superleaks  $S_1$ ,  $S_2$  and  $S_3$ , two heat exchangers  $W_1$  and  $W_2$  and the all-important capillary C, all connected in series. The heat exchangers are sintered-copper cylinders embedded in the copper block of the  $^3\text{He}$  refrigerator. The function of the superleaks  $S_1$  and  $S_3$  is to introduce  $^4\text{He}$  into the flow system  $W_1$ - $S_2$ -C- $W_2$  without introducing the heat content of the  $^4\text{He}$ . Therefore only a modest reservoir of  $^3\text{He}$  is needed to cool the flow system to the desired starting temperature. The superleaks are made by compressing jeweller's rouge into stainless-steel capillaries of 1.0 mm i.d., 1.45 mm o.d.

The capillary is of the same type as the one used in earlier experiments<sup>4)</sup>, made of stainless-steel 100  $\mu\text{m}$  i.d., 200  $\mu\text{m}$  o.d., having a free length of 48.2 cm. For compactness it is wound into a spiral of 1 cm diameter  $\times$   $\approx$  10 cm. Five Allen-Bradley thermometers are connected via thin copper strips at roughly equal intervals along the capillary. The first thermometer,  $T_1$ , is actually soldered to a small copper tube Ch, connecting  $S_2$  to the capillary. A calibrated Ge thermometer,  $T_{\text{BL}}$ , is used to read the temperature of the  $^3\text{He}$  block and for calibrating the thermometers. A separate carbon thermometer (not shown in the figure) and a heater were used to regulate the temperature of the  $^3\text{He}$  block to within 1 mK. The system  $W_1$ - $S_2$ -C- $W_2$  in fig. 2 is analogous to the system reservoir-superleak-capillary-bath in fig. 1, with the advantage that the "reservoir" ( $W_1$ ) and "bath" ( $W_2$ ) in fig. 2 can be held at temperatures from  $T_\lambda$  down to 0.3 K. The pressure head applied on the whole system in fig. 2,  $\Delta Z$  (cm He) is equal to the pressure difference over  $S_2$ -C, because the fountain-pressure drops over  $S_1$  and  $S_3$  are equal. The whole system has been designed so that no critical flow

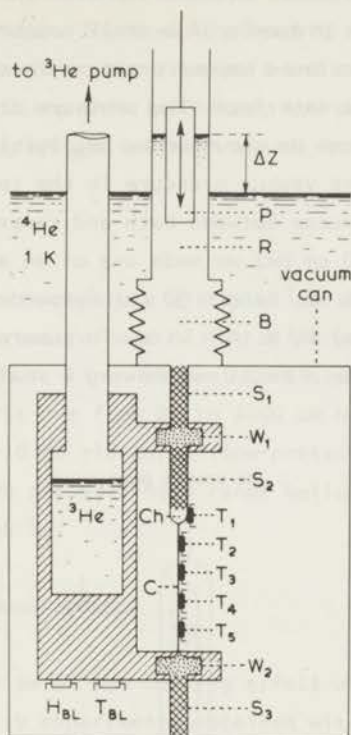


Fig. 2. Schematic diagram of the apparatus. (P) plunger, (R) reservoir, (B) bellows, (S) superleaks, (W) heat exchangers, (Ch) chamber, (C) capillary, (T) thermometers, (H) heater.

rates will be reached elsewhere until the velocity in C is about 100 times the critical velocity. Two different arrangements were used for generating the pressure head  $\Delta Z$ . For the high positive pressure heads (20 to 2000 cm He) we employed the type used in earlier experiments <sup>4)</sup> which is depicted in fig. 3. The reservoir R and capillary C', both made of glass, are thermally isolated from the main helium bath by a glass vacuum mantle. The reservoir can be partially filled via a superfluid-leak-tight beryllium-copper valve <sup>7)</sup> V, connected to a copper bellows B, which acts as a heat exchanger. The helium in the reservoir can be heated by a heater H to a temperature higher than that of the main bath. The pressure in the reservoir is then determined from the vapour

pressure above the liquid, using the thermometer T to measure the liquid temperature. Assuming temperature equilibrium over the length of the reservoir (which is aided by the presence of a small copper rod running the length of the reservoir), the calculated vapour pressure is the exact pressure in the liquid at the liquid-vapour interface. The pressure drop over the capillary C' due to the flow of helium can be shown to be negligibly small. The pressure head  $\Delta Z$  then is equal to the vapour pressure in the reservoir plus or minus the hydrostatic pressure difference between bath and reservoir level. For the low-pressure heads (-10 to +10 cm He) we made use of an arrangement consisting of a solid plunger (diameter 5 mm, length 30 cm) suspended in a glass tube (inner diameter 7 mm, length 70 cm) by a thin wire. To suppress film flow the top of the glass tube was sealed by a metal cap having a small hole through which the

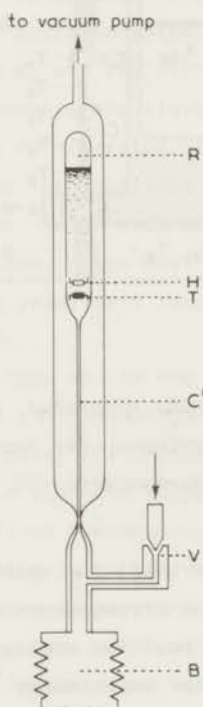


Fig. 3. The high-pressure head generator. (R) reservoir, (H) heater, (T) thermometer, (C') capillary (i.d. = 1.0 mm,  $l$  = 22 cm), (V) valve, (B) bellows.



wire passed. This wire was attached to a rod which passed through a vacuum seal in the top of the cryostat and which could be moved with constant velocities by a motor-driven gear system. The pressure head  $\Delta Z$  is the hydrostatic pressure difference between the levels in the reservoir and main bath, which is read by means of a cathetometer. Using this technique, low-pressure heads could be held constant for a period long enough to reach steady conditions.

### 3. *Experimental results*

We have measured the temperature distribution along the capillary as a function of the applied pressure head  $\Delta Z$  for different combinations of starting temperatures at  $W_1$  and  $W_2$ . It is convenient to distinguish between two regimes of pressure head; the first one from 20 to 2000 cm He (high-pressure heads) and the second one from -10 to +10 cm He (low-pressure heads). It should be noted that in the negative pressure-head range helium flows through the capillary towards the superleak  $S_2$ .

#### 3.1. *High-pressure head measurements*

To give an overall view of the cooling effect we present in fig. 4 the results of two of our early experiments obtained with the end of the capillary C directly coupled to the main  $^4\text{He}$  bath at 1.04 K ( $W_2$  and  $S_3$  bypassed). This was necessary because when helium flows under high-pressure heads (and thus at high dissipation levels) a considerable amount of heat emerges from the end of the capillary and it becomes difficult to maintain the  $^3\text{He}$  block at a low temperature. The solid symbols represent data points taken with the  $^3\text{He}$  block (hence  $W_1$ ) at 0.3 K. In spite of the fact that there is now a heat leak over the superleak  $S_2$  in the direction of  $W_1$ , the lowest temperature reached in the chamber, Ch, is still 0.77 K at very high pressure heads, i.e., about 2000 cm He (not shown in fig. 4). Since this temperature can be due neither to the heat leak over  $S_2$  nor to the imperfection of the superleak itself, we are led to the conclusion that the limiting temperature of about 0.75 K in our capillary is due to the intrinsic properties of the helium flowing through the capillary.

In order to investigate whether cooling occurs at all starting temperatures of  $T_1$ , one would like to carry out a series of measurements at an overall starting temperature of less than 0.75 K. We achieved this (again bypassing  $W_2$  and  $S_3$ ) in the following way. The capillary was thermally anchored to the  $^3\text{He}$  block over a length of about 1 cm at a point midway between  $T_3$  and  $T_4$  (see

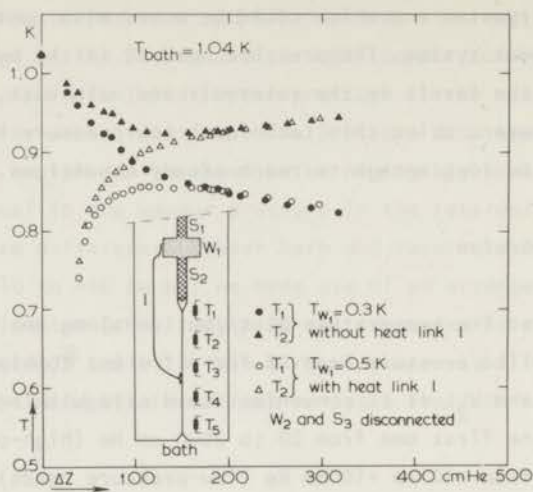


Fig. 4. The temperatures  $T_1$  and  $T_2$  as functions of the applied pressure head  $\Delta Z$  in the high-pressure head region at two different starting temperatures.

insert of fig. 4). This was sufficient to cool the portion of the capillary between  $S_2$  and  $T_3$  to 0.5 K, while the lower portion of the capillary was at bath temperature, 1.04 K. The open symbols in fig. 4 represent data of  $T_1$  and  $T_2$  obtained with this arrangement, which can be seen to join smoothly onto the previous set of data at pressure heads of  $\approx 200$  cm He (1 atm  $\approx 7000$  cm He). This demonstrates the fact that the lowest temperature attainable at high-pressure heads is independent of the starting temperature. In addition, since the effective length of the capillary is not the same for both sets of data, we see that the limiting temperature is independent of the length of the capillary.

One can still ask whether cooling could occur at a starting temperature of 0.5 K at low-pressure heads, i.e., of the order of the maximum possible fountain pressure over the superleak (about 1.2 cm He). In view of this we have investigated in more detail the low-pressure head regime.

### 3.2. Low-pressure head measurements

The low-pressure head measurements were performed in the apparatus sketched

in fig. 2, with  $W_2$  and  $S_3$  being reinstalled.

When helium was allowed to flow under these low-pressure heads, at a starting "reservoir" temperature of 0.5 K, no cooling was detected, for positive as well as for negative pressure heads (in the latter case no cooling could be expected). On the contrary, a steady rise of the temperature of the cooling chamber was observed as the absolute magnitude of the pressure head was increased. The temperature distribution over the capillary was found to be almost parabolic when the temperatures of the five thermometers were plotted as functions of their distances from the chamber (see fig. 5). This almost parabolic profile suggests that there is homogeneous dissipation occurring in the capillary and that the temperature distribution in the flowing He II can be described with an effective coefficient of thermal conductivity  $K$ , completely analogous to the problem of the temperature distribution in a finite rod within

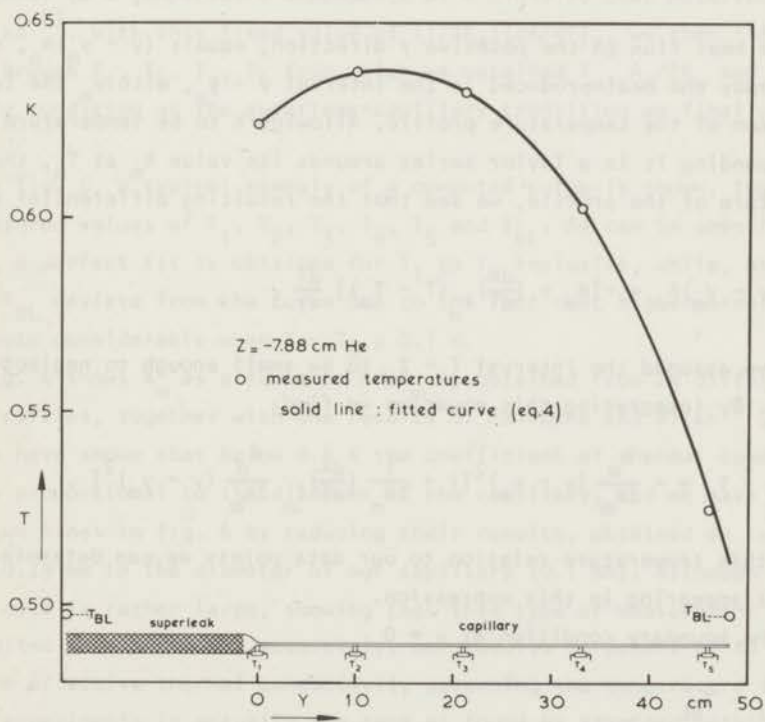


Fig. 5. Temperature distribution over the capillary in the low-pressure head region.  $\circ$  measured temperatures. The solid line represents the fit according to eq. (4).



which: i) heat is being produced homogeneously at the constant rate of  $A_0$  ( $W\text{ cm}^{-3}$ ), ii) where there is no radial heat flow, iii) where one end of the rod is maintained at the constant temperature  $T_{BL}$ , and iv) where the other end is attached to a reservoir at temperature  $T_m$  via a thermal link of small but finite conductivity (i.e. a heat leak). In our case the heat link is the superleak  $S_2$ , the rod is the column of helium and the only complication is that this helium is encapsulated by a metal capillary within which no heat is being generated. Fortunately the heat conduction by the capillary itself can be neglected owing to the enormous difference in the thermal conductivity of stainless steel and He II.

Treating this situation as a heat-conduction problem we have to solve the equation

$$\dot{q} = -K \frac{dT}{dy} \quad (2)$$

where  $\dot{q}$ , the heat flux in the positive  $y$  direction, equals  $(y - y_m)A_0$ , since it carries away the heat produced in the interval  $y - y_m$ , with  $y_m$  the location of the maximum of the temperature profile. Allowing  $K$  to be temperature dependent and expanding it in a Taylor series around its value  $K_m$  at  $T_m$ , the maximum temperature of the profile, we see that the resulting differential equation reads

$$(y - y_m)A_0 = -[K_m + \left(\frac{dK}{dT}\right)_{T_m} (T - T_m)] \frac{dT}{dy}, \quad (3)$$

where we have assumed the interval  $T - T_m$  to be small enough to neglect higher-order terms. By integrating this equation we find:

$$T - T_m = -\frac{A_0}{2K_m} (y - y_m)^2 \left[1 + \frac{1}{2K_m} \left(\frac{dK}{dT}\right)_{T_m} \frac{A_0}{2K_m} (y - y_m)^2\right]. \quad (4)$$

By fitting this temperature relation to our data points we can determine the coefficients appearing in this expression.

From the boundary condition at  $y = 0$

$$\frac{T_1 - T_{BL}}{R_0 c} = A_0 y_m \quad (5)$$

and the value of  $y_m$  we can determine the dissipation rate  $A_0$ , and from that  $K_m$ . In this boundary condition  $R$  is the thermal resistance of the superleak which in a separate experiment was found to be  $8.4 \times 10^6 \text{ K W}^{-1}$ , and  $0_c$  is the cross-sectional area of the capillary. The systematic error introduced in the

analysis by neglecting higher-order terms in eq. (3) can be shown to be small by assuming a temperature dependence of  $K$  similar to that observed by Fairbank and Wilks<sup>8)</sup> and by restricting the temperature region to the vicinity of the top of the temperature profile between the thermometers  $T_1$  and  $T_4$  where  $T - T_m$  never exceeds 40 mK.

In principle, from the four temperatures  $T_1, T_2, T_3$  and  $T_4$  one could determine the four coefficients  $T_m, A_0/2K_m, \gamma_m$  and  $(1/2K_m)(dK/dT)_{T_m}$  exactly. However, the limited measuring accuracy does not permit us to apply this procedure because it can lead to a prohibitively large value of the correction term in eq. (4). Due to the scarcity of data points this term is very sensitive to the exact values of  $T_1, T_2, T_3, T_4$ . Therefore we cannot determine the temperature dependence of  $K$  from each individual temperature profile. To keep the correction term reasonably small, we have set  $(1/2K_m)(dK/dT)_{T_m} \equiv 2.5$ , which corresponds to a temperature dependence of  $K$  close to that observed by Fairbank and Wilks<sup>8)</sup>. With this fixed value of  $(1/2K_m)(dK/dT)_{T_m}$  we then fitted the best curve through  $T_1, T_2, T_3, T_4$  from which we obtained  $T_m, A_0/2K_m$  and  $\gamma_m$ . With the boundary condition at the superleak-capillary transition we finally find  $A_0$  and  $K_m$ .

In fig. 5, a typical example of a computed curve is shown, together with the measured values of  $T_1, T_2, T_3, T_4, T_5$  and  $T_{BL}$ . As can be seen from this figure, a perfect fit is obtained for  $T_1$  to  $T_4$  inclusive, while, as expected,  $T_5$  and  $T_{BL}$  deviate from the curve due to the fact that higher-order terms do contribute considerably when  $T - T_m \approx 0.1$  K.

Fig. 6 shows  $K_m$  as a function of  $T_m$  as obtained from 24 different temperature profiles, together with the results of Fairbank and Wilks<sup>8)</sup>. These authors have shown that below 0.6 K the coefficient of thermal conductivity is roughly proportional to the diameter of the capillary, and we have obtained the drawn lines in fig. 6 by reducing their results, obtained on tubes of 0.8 mm and 0.29 mm to the diameter of our capillary (0.1 mm). Although the scatter in our data is rather large, showing that this type of measurement is not very well suited to determine  $K$  accurately, our results do permit us to conclude that the effective thermal conductivity governing the temperature distribution in our experiments is actually the same as found by standard methods. Our main conclusion from these measurements of the temperature distribution therefore is that, below 0.75 K, the flow of helium is not accompanied by a convective heat transport, so that below this temperature the cooling effect no longer exists.

The results for  $A_0$  are shown as a function of the applied pressure head  $\Delta Z$  in fig. 7. Even in the case that  $\Delta Z = 0$ , we still found a temperature

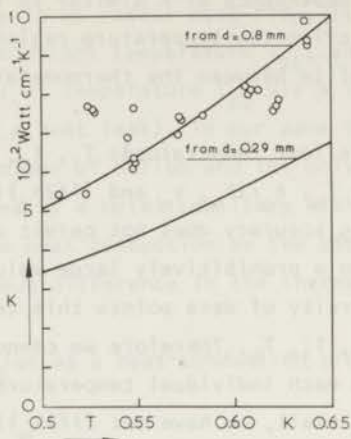


Fig. 6. The coefficient of thermal conductivity as a function of temperature. O effective coefficient of thermal conductivity as calculated from the temperature profile. The solid lines are the results of Fairbank and Wilks reduced to the diameter of 0.1 mm.

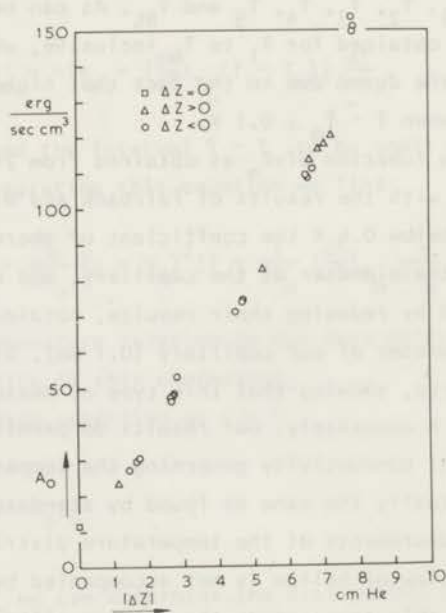


Fig. 7. The energy dissipation rate  $A_0$  as a function of the applied pressure head.

profile, and consequently a value of  $A_O^D (\equiv A_O^V)$ , which we ascribe to heat input due to vibrations of the capillary. Although the capillary was supported by a socket made of thin cigarette paper, the system was still loosely suspended and easily brought into resonant vibrational modes. Due to the low heat capacity of the system near 0.5 K such vibrational modes gave considerable warming. The heat input due to the dissipation of the helium,  $A_O^D = A_O - A_O^V$ , is shown in fig. 8, where we have assumed  $A_O^V$  to be the same for all pressure heads. This assumption seems reasonable in view of the fact that the points at non-zero pressure head join smoothly onto the zero pressure head value. Fig. 8 suggests that  $A_O^D$  is proportional to  $|\Delta Z|^{4/3}$ . On the other hand we can compute  $A_O^D$  from the measured values of  $v_s$  (the superfluid velocity in the capillary) and  $\Delta Z$ . The total energy dissipated into the capillary through which He II flows at a velocity  $v$ , and over which there exists a difference in chemical potential  $\Delta\mu$ , is equal to  $\rho_c v \Delta\mu$ . From this follows

$$A_O^D = \rho_s v_s g \Delta Z / \ell \quad , \quad (6)$$

where  $g$  is the acceleration due to gravity and  $\ell$  the length of the capillary.

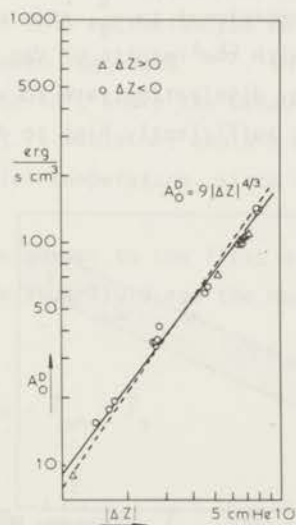


Fig. 8. The energy dissipation rate corrected for the vibrational heat input as a function of the applied pressure head. Solid line  $4/3$  power; dashed line  $3/2$  power.



However, in this experiment it proved to be difficult to obtain reliable values of  $v_s$  at a given  $\Delta Z$  because these had to be calculated from the flow rate out of or into the reservoir. Since in the actual experiment the reservoir is open on top, the evaporation of the helium in the reservoir has to be taken into account, which unfortunately is dependent on the position of the plunger in the reservoir. Therefore  $v_s$  has been calculated from the measured values of  $A_O^D$ , using eq. (6). These values of  $v_s$  can then be compared with values obtained experimentally in a slightly different but more reliable way than those from the plunger experiment. With the arrangement used in our high-pressure head measurements we could also produce level differences from -10 to +10 cm He, which, however, could not be kept constant in time, as the reservoir was gradually filled from or emptied into the bath. By monitoring the levels in the reservoir and of the bath we were able to calculate at each level difference the velocity in the capillary. The results obtained in this way differed from day to day, but all are within the shaded area in fig. 9. It is reassuring to see that most of the  $v_s$  values deduced from  $A_O^D$  are within this region, supporting our earlier conclusion that no heat is carried away by convective heat transport at temperatures below 0.75 K. Finally, the results shown in fig. 8 seem to be better described by the relation  $A_O^D \sim |\Delta Z|^{4/3}$  which would imply that the energy dissipation rate is proportional to  $v_s^4$ , than by the relation  $A_O^D \sim |\Delta Z|^{3/2}$  which, in accordance with the results of Van Alphen<sup>9)</sup>, would lead to a proportionality of the energy dissipation rate to  $v_s^3$ . Unfortunately, the accuracy of our results is not sufficiently high to determine the exact power

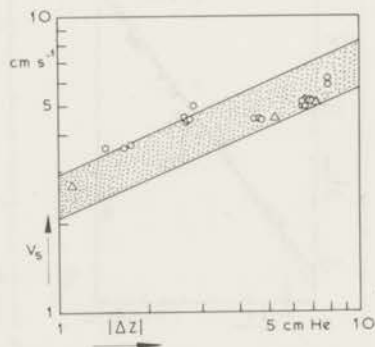


Fig. 9. The superfluid velocity as a function of the applied pressure head as calculated from eq. (6) compared with directly measured values of  $v_s$ .

involved, as can be seen from fig. 8, where the two lines  $A_0^D \sim |\Delta Z|^{4/3}$  and  $A_0^D \sim |\Delta Z|^{3/2}$  are drawn.

#### 4. Discussion

In review, we have seen that the heat leak through the superleak is not responsible for the limiting temperature being about 0.75 K. Furthermore, we have seen that at a starting temperature of 0.5 K, even at the lowest measured pressure heads, there is no discernible cooling in our apparatus. Similar measurements at starting reservoir temperatures of 0.6, 0.7 and 0.8 K show that only in the vicinity of 0.8 K does cooling by convective heat transport set in. (See also fig. 4.)

We conclude that the simple explanation, put forward in the introduction, needs at least to be extended in order to describe all the phenomena observed. For instance, if for stationary flow during cooling the pressure difference over the capillary,  $\Delta P_c$ , is zero, what force prevents the normal excitations to flow back to the chamber in the presence of the then existing temperature gradient in the capillary? Secondly, what is the mechanism responsible for the occurrence of the limiting temperature now that heat leaks from the bath can be excluded? In our opinion this mechanism can not simply be the dissipation becoming dominant, as has been suggested<sup>4,5)</sup>. In that case such a flat minimum as observed in figs. 10<sup>a</sup> and 10<sup>b</sup>, where the behaviour of  $T_a$  is shown, would be very unlikely. Furthermore, it would not explain why the limiting temperature is independent of the initial temperature, since quite different dissipation levels are involved.

In order to obtain the answer to the first question we will consider the equations of motion for the superfluid and the normal component, which are usually written as<sup>15)</sup>

$$\rho_s \frac{d\vec{v}_s}{dt} = -\rho_s \vec{\nabla} \mu - \vec{F}_{sn} - \vec{F}_s \quad (7)$$

$$\rho_n \frac{d\vec{v}_n}{dt} = -\frac{\rho_n}{\rho} \vec{\nabla} P - \rho_s s \vec{\nabla} T + \vec{F}_{sn} - \vec{F}_n \quad (8)$$

where  $\vec{v}_s$  and  $\vec{v}_n$  are the transport velocities of the superfluid and normal components and  $s$  the entropy per gram. If the heat leak through the superleak and through the liquid itself as well as the dissipation in the capillary are neglected, the normal fluid velocity  $\vec{v}_n$  will be zero in the steady state and the

equations reduce to:

$$0 = -\rho_s \vec{\nabla} \mu - \vec{F}_{sn} - \vec{F}_s \quad (9)$$

$$0 = -\frac{\rho_n}{\rho} \vec{\nabla} P - \rho_s s \vec{\nabla} T + \vec{F}_{sn} \quad (10)$$

Were the pressure difference over the capillary,  $\Delta P_c \neq 0$  and alone responsible for the cooling, the mutual friction force  $\vec{F}_{sn}$  being zero, it would follow from eqs. (9) and (10) that  $\vec{\nabla} P = -\vec{F}_s$  and that the temperature difference would be governed by

$$T_a = T_{\text{bath}} - \frac{g\Delta Z}{s_\lambda} \quad (11)$$

where we have assumed  $\rho_n/\rho = s/s_\lambda$ , with  $s_\lambda$  the entropy per gram of liquid at the lambda temperature.

In fig. 10<sup>a</sup> the straight line given by eq. (11) is drawn, together with a measured cooling run. Obviously our data do not obey this relation. For each run we have also plotted in figs. 10<sup>a</sup> and 10<sup>b</sup> the line corresponding to a zero pressure difference over the capillary, i.e.,  $\vec{F}_s = 0$ , which leads to

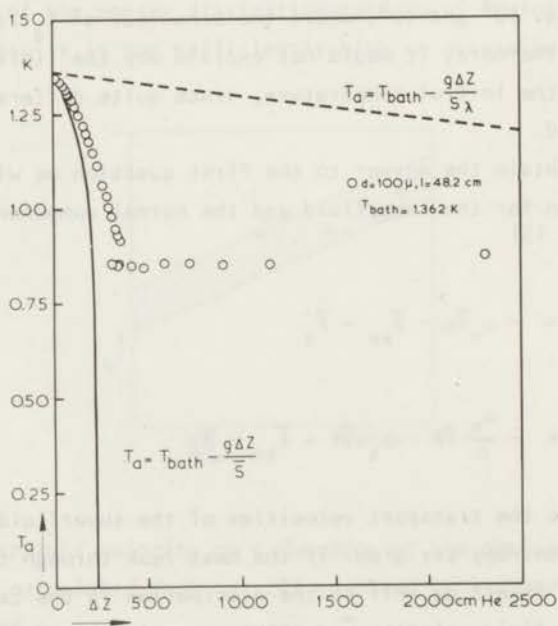
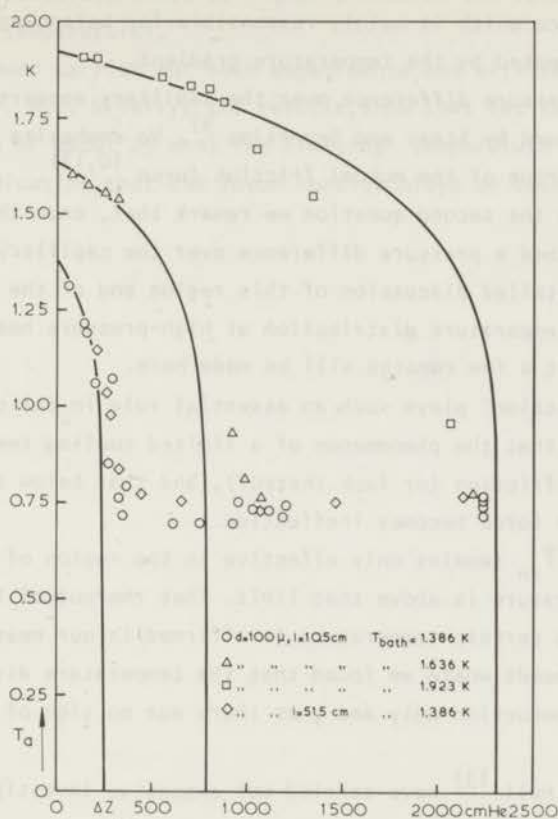


Fig. 10a.

Fig. 10b.



Figs. 10a and b.  $T_a$  as a function of the applied pressure head at different starting temperatures. The dashed line in fig. 10a is calculated under the assumption that  $\vec{F}_{sn} = 0$ . The solid lines in figs. 10a and 10b correspond to a zero pressure difference over the capillary.

$$T_a = T_{\text{bath}} - g\Delta Z/\bar{s} \quad (12)$$

(the well-known London equation for the superleak), where  $\bar{s}$  is the entropy per gram of liquid averaged over the temperature interval  $T_a - T_{\text{bath}}$ .

As long as the limiting temperature is not reached our data seem to be in fair agreement with the latter expression. The deviations correspond to a small pressure difference over the capillary and can be due either to  $\vec{F}_s \neq 0$  or to  $\vec{v}_n \neq 0$  the latter of which would account for dissipation and heat leaks.



However, the deviations are generally small and we can conclude that it is the mutual friction force which is mainly responsible for balancing the force on the normal fluid created by the temperature gradient.

Indeed, the pressure difference over the capillary appears to be close to zero, as was argued by Staas and Severijns <sup>5)</sup>. We emphasize that this is only achieved by virtue of the mutual friction force <sup>10,11)</sup>.

With regard to the second question we remark that, once the limiting temperature is reached a pressure difference over the capillary arises. We shall postpone a detailed discussion of this region and of the information we gathered from the temperature distribution at high-pressure heads until a subsequent chapter, but a few remarks will be made here.

As "mutual friction" plays such an essential role in the cooling process, it seems plausible that the phenomenon of a limited cooling temperature is also a result of mutual friction (or lack thereof), and that below this temperature the mutual friction force becomes ineffective.

It seems that  $\vec{F}_{sn}$  remains only effective in the region of the capillary in which the temperature is above that limit. That the mutual friction becomes ineffective below a certain temperature is affirmed in our measurements at 0.5 K at low-pressure heads where we found that the temperature distribution was governed by heat conduction only and that there was no sign of convective heat transport.

Vinen <sup>12)</sup> and Hall <sup>13)</sup> have carried out extensive investigations concerning the mutual friction force.

It is currently believed that interaction between the superfluid and the normal fluid takes place via vortex lines or rings. The total "friction" force  $\vec{F}_{sn} + \vec{F}_s$  corresponds to the momentum which is extracted from the superfluid transport and stored in the system of vortices. Part of this momentum ( $\vec{F}_{sn}$ ) is transferred to the normal component by interaction of the vortices with the excitations. Since there are two different kinds of excitations - phonons and rotons - it is intriguing to find out whether the interaction is equally effective on both. Rayfield and Reif <sup>14)</sup> have shown that the rotons are much more drastically scattered by vortex rings than are phonons.

The limiting temperature of about 0.75 K now strikes us as a peculiar one, since only above this temperature do rotons begin to appear in detectable numbers (cf. the specific heat).

Our results seem to suggest that cooling takes place mainly because of the interaction between vortices and rotons. If the roton density is related to the limiting temperature it would be of interest to extend our experiments to

higher overall pressures, since at higher pressures the rotons manifest themselves at lower temperatures.

We have indeed carried out such experiments and will report on them in the next chapter. But, briefly, the results show that (at the highest overall pressure of about 25 atm) the limiting temperature is lowered by about 0.1 K, indicating that the roton density plays an essential role in the cooling process.

## References

- 1) Daunt, J.G. and Mendelssohn, K., *Nature* 143 (1939) 719.
- 2) Simon, F.E., *Physica* 16 (1950) 753.
- 3) Kapitza, P., *J. Phys. U.S.S.R.* 5 (1941) 59; *Phys. Rev.* 60 (1941) 354.
- 4) Olijhoek, J.F., van Alphen, W.M., De Bruyn Ouboter, R. and Taconis, K.W., *Physica* 35 (1967) 483.
- 5) Staas, F.A. and Severijns, A.P., *Cryogenics* 9 (1969) 422.
- 6) Bots, G.J.C. and Gorter, C.J., *Physica* 22 (1956) 503 (*Commun. Kamerlingh Onnes Lab., Leiden No. 304b*).
- 7) Hoffer, J.K., Ph. D. Thesis, Berkeley, (1968).
- 8) Fairbank, H.A. and Wilks, J., *Proc. Roy. Soc. A* 231 (1955) 545.
- 9) Van Alphen, W.M., De Bruyn Ouboter, R., Taconis, K.W. and De Haas, W., *Physica* 40 (1969) 469 (*Commun. Kamerlingh Onnes Lab., Leiden No. 367a*).
- 10) Staas, F.A. and Taconis, K.W., *Physica* 27 (1961) 924.
- 11) Staas, F.A. and Severijns, A.P., *Proceedings of the Third International Cryogenic Engineering Conference, Berlin* (1970) 320.
- 12) Vinen, W.F., *Proc. Roy. Soc. A* 260 (1961) 218.
- 13) Hall, H.E., *Phil. Mag. Suppl.* 9 (1960) 89.
- 14) Rayfield, G.W. and Reif, F., *Phys. Rev.* 136A (1964) 1194.
- 15) See for instance Wilks, J., *The Properties of Liquid and Solid Helium*, Clarendon Press (Oxford, 1967) Chapter 13.



## CHAPTER II

### MEASUREMENTS AT HIGH OVERALL PRESSURE; THE MUTUAL FRICTION FORCE AND THE INFLUENCE OF PRESSURE ON THE LIMIT FOR COOLING

#### *Synopsis*

In continuation of our investigations on the cooling effect which occurs when He II is forced to flow under adiabatic conditions through a system consisting of a superleak, a chamber and a capillary in series measurements on the flow of He II under high overall pressures are reported.

It is found that as expected the limiting temperature for cooling of about 0.75 K does indeed decrease with increasing overall pressure, occurring at a fixed roton density.

The occurrence of this limit appears to be a complicated phenomenon, in which the roton density as well as dissipation by the flow, either in the chamber or in the capillary, seems to play an essential role.

In the present apparatus the velocities of the normal and superfluid components could be varied independently in a wide range of velocities, enabling us to study the nature of the all important mutual friction force. It is found that a mutual friction force of the Gorter-Mellink type, i.e.,

$F_{sn} = A\rho_s\rho_n(v_s - v_n)^3$  gives an adequate description of the behaviour of the chamber temperature at sufficiently low velocities.

#### 1. Introduction

In the preceding chapter <sup>1)</sup> it has been shown that cooling by convective heat transport in helium II, as can be obtained by driving helium II through a flow system consisting of a superleak connected to the helium bath via a chamber and a narrow capillary (see fig. 1), is dominated by the "mutual friction" between the superfluid and the normal component. The temperature in the chamber,  $T_a$ , at the upstream side of the capillary was found to be well described by the relation

$$\int_{T_a}^{T_{\text{bath}}} s dT = - \Delta\mu \quad (1)$$

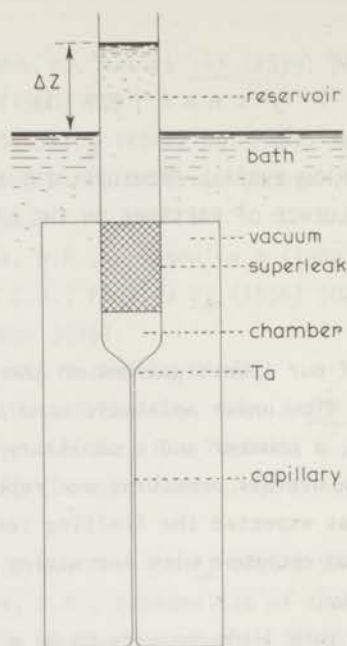


Fig. 1. Diagram of the basic parts of the cooling device.

where  $s$  is the entropy per gram of liquid helium II and  $-\Delta\mu$  the chemical potential difference applied to the flow system by means of a pressure head  $\rho g\Delta Z = -\rho\Delta\mu$  (see fig. 1). This relation shows that in the stationary state the force on the normal component due to the temperature gradient in the capillary is balanced by a mutual friction force rather than by a pressure gradient. Once a temperature of  $T_a$  as low as  $\approx 0.75$  K has been reached, relation (1) appears to be no longer obeyed, when  $\Delta\mu$  is further increased. Independent of the bath temperature 0.75 K seems to be the lower limit for this cooling method; at bath temperatures below 0.75 K no cooling has ever been detected, on the contrary a warming up is observed. It has been shown that this limit is not due to heat leaks from the bath and it has been suggested that this limiting temperature is connected to the roton density in helium II, through which the "mutual friction force" should be effective and which becomes too small at temperatures below 0.75 K. <sup>1)</sup>

If the roton density, which increases with pressure is indeed responsible for the limiting temperature of  $T_a$ , one could expect a lowering of this limit with increasing pressure. In order to investigate this we have constructed an

apparatus by means of which cooling curves can be measured at higher overall pressures ranging to 25 atm. In addition, since the apparatus is constructed in such a way that the normal and the superfluid flow velocities are adjustable independently in a wide range of velocities, the nature of the mutual friction force can be studied.

## 2. Experimental set-up

A schematic diagram of the experimental set-up is shown in fig. 2. Helium

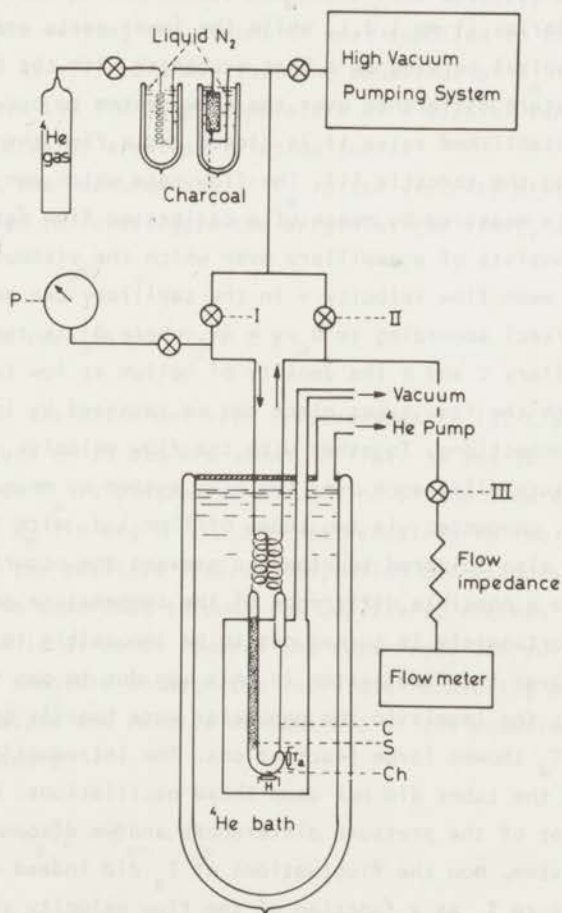


Fig. 2. Schematic drawing of the experimental set-up. (S) superleak, (Ch) chamber, (C) capillary, (H) heater, (T<sub>a</sub>) thermometer, (I) inlet valve, (III) outlet valve.



at high pressure is introduced into the cryostat from a storage cylinder at room temperature after flowing through two cold traps. The flow system, which is contained in a vacuum can, consists again of a superleak S (i.d. 1 mm, length 11 cm) connected via a copper chamber Ch (which is actually a bended copper tube with an inner diameter of 1 mm and a length of 1 cm) to a stainless steel capillary C (i.d. 208  $\mu\text{m}$  with a length of 10.4 cm). Special care was taken to make a smooth change-over of diameter between the chamber and the much narrower capillary. From this flow system two connections lead to the top of the cryostat. They are soldered together along their entire lengths so that the outflow precools the inflow of helium. The upper part of these tubes are stainless steel capillaries (1 mm i.d.), while the lower parts are copper tubes wound together into a spiral serving as a heat exchanger with the bath, in order to prevent a temperature difference over the flow system to occur. Once temperature equilibrium is established valve II is closed and a flow through the system is started by opening the throttle III. The flow rate which can be regulated by this same valve is measured by means of a calibrated flow meter at room temperature which consists of a capillary over which the viscous pressure difference is measured. The mean flow velocity  $v$  in the capillary can be deduced from this flow rate  $\dot{V}$  (mol/sec) according to  $0_c \rho v = 4\dot{V}$ , where  $0_c$  is the cross-sectional area of the capillary C and  $\rho$  the density of helium at low temperature. The direction in which the flow takes place can be reversed by interchanging the in- and outlet connections. Together with the flow velocity  $v$  we intended to measure the pressure difference over the flow system by means of a differential mercurymanometer, connected via two tubes of 1 mm i.d. with the flow system. These tubes were also soldered together to prevent the occurrence of a pressure difference due to a possible difference of the temperature gradients in both capillaries. Unfortunately it turned out to be impossible to measure the pressure difference over the flow system in this way due to gas vibrations in the connecting tubes; the levels in the manometer were heavily oscillating and even the temperature  $T_a$  showed large fluctuations. The introduction of very narrow constrictions in the tubes did not damp these oscillations. We therefore gave up the measurement of the pressure differences and we disconnected the manometer from the flow system. Now the fluctuations of  $T_a$  did indeed disappear and we were able to measure  $T_a$  as a function of the flow velocity  $v$  only. The overall pressure was read on the manometer P which had a range of 40 atm (Schäfer & Budenberg). With the help of the heater H we were able to adjust a flow velocity of the normal component in the capillary independently of the total mass flow velocity  $v$ . The temperature at the chamber,  $T_a$ , was measured by an Allen and

Bradley resistance thermometer,  $\frac{1}{10}$  W, nominal resistance 10  $\Omega$ . A bridge voltage of 0.5 mV was employed in order to reduce heat production in the thermometer.

The bridge output was amplified by a Keithley 150 B voltmeter and displayed on a Solartron LM 1420.2 digital voltmeter and on a chart recorder.

### 3. *Experimental results*

The temperature at the chamber,  $T_a$ , is measured as a function of the flow velocity  $v$ . These measurements are carried out at different overall pressures and at different values of the normal component flow velocity which is varied independently of  $v$  by varying the amount of heat supplied to the chamber.

In section 3.1 it will be shown that the behaviour of  $T_a$  in the region above 1 K (well above the limiting temperature of  $\approx 0.75$  K) can successfully be interpreted in terms of a mutual friction force.

In section 3.2 the measurements of  $T_a$  in the vicinity of the limiting temperature, intended to investigate the origin of the limit, are presented and discussed.

#### 3.1. *Analysis of the results for $T_a > 1$ K*

The results for two different bath temperatures (1.152 K and 1.455 K) both at an overall pressure of 10 atm are shown in figs. 3a and 3b.

In these figures  $T_a$  is plotted as a function of the flow velocity  $v$  for different values of  $\dot{Q}_H$  (in  $\text{erg s}^{-1}$ ), the heat supplied to the chamber by means of the heater H. In the positive  $v$ -direction, which corresponds to cooling, helium flows from the superleak through the capillary, whereas in the negative  $v$ -direction the flow is directed towards the superleak. The curves in figures 3a and 3b are drawn smoothly through the individual measuring points.

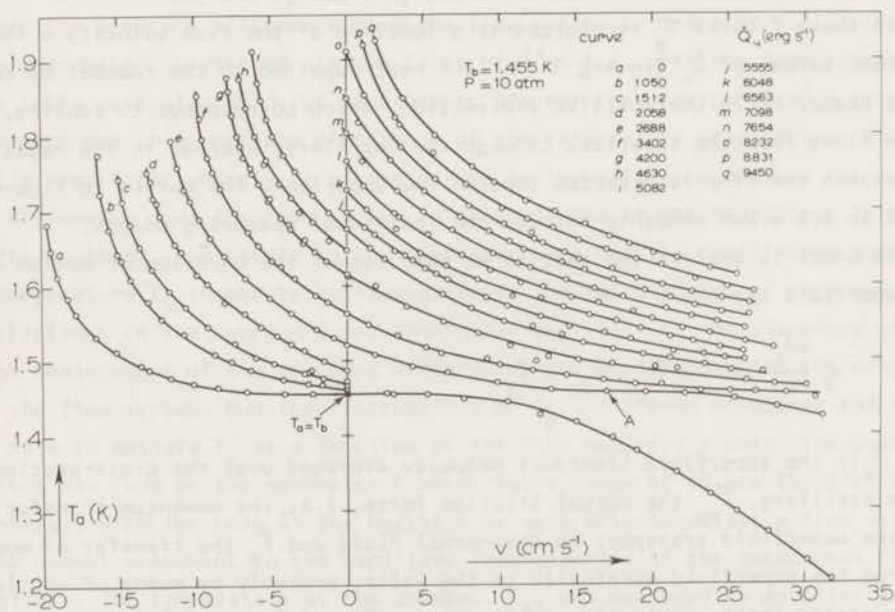
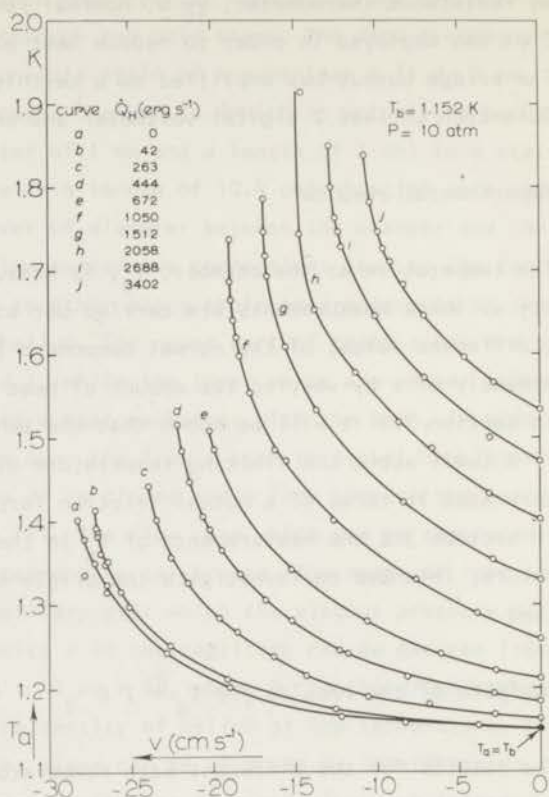
In order to analyse the results we make use of the equation of motion for the superfluid transport

$$\rho_s \frac{d\vec{v}_s}{dt} = -\rho_s \vec{\nabla}\mu - \vec{F}_{sn} - \vec{F}_s \quad (2)$$

where  $\vec{v}_s$  is the superfluid transport velocity averaged over the cross-section of the capillary,  $\vec{F}_{sn}$  the mutual friction force, i.e., the momentum transfer from the superfluid transport to the normal fluid and  $\vec{F}_s$  the transfer of momentum from the superfluid eventually to the walls, probably by means of vortices. In the steady state, neglecting gradients in  $v_s^2$  and  $v_n^2$ , eq. (2) for the transport



Fig. 3a and 3b.  $T_a$  as a function of the net mass flow velocity at various heat inputs.



direction reduces to:

$$0 = -\frac{\rho_s}{\rho} \frac{dP}{dx} + \rho_s s \frac{dT}{dx} - F_{sn} - F_s \quad (3)$$

From the transport of the normal component one obtains under the same conditions:

$$0 = -\frac{\rho_n}{\rho} \frac{dP}{dx} - \rho_s s \frac{dT}{dx} + F_{sn} - F_n \quad (4)$$

where given the type of normal flow (e.g. laminar)  $F_n$  as a function of the averaged transport velocity  $v_n$  can be derived from  $-F_n = \eta_n \nabla^2 v_n$ , where  $-F_n$  the viscous force on the normal component with  $\eta_n$  the viscosity and  $v_n$  the local velocity of the normal fluid.

From equations (3) and (4) it follows that

$$-\frac{dP}{dx} = F_s + F_n \quad (5)$$

In view of the results described in a previous paper <sup>1)</sup>, where it is found that in the capillary  $\frac{dP}{dx}$  is small compared to  $\rho \frac{d\mu}{dx}$ , for appreciable values of  $\frac{d\mu}{dx}$ , we will attempt to analyse the results obtained at high pressure, as given in figs. 3a and b, also by neglecting  $\frac{dP}{dx}$  in the region where  $\frac{d\mu}{dx}$  is appreciably different from zero, in which case equations (3) and (4) reduce to

$$0 = -\rho_s s \frac{dT}{dx} + F_{sn} \quad (6)$$

The question now remains whether a form for  $F_{sn}$  as a function of temperature and of the averaged velocities  $v_s$  and  $v_n$  can be found which correctly describes all the results for the different types of adiabatic flow given in figs. 3a and b in terms of equation (6).

It should be noted that the entropy  $s$  and the densities ( $\rho$ ,  $\rho_s$ ,  $\rho_n$ ) at a given temperature are dependent on the overall pressure. In our numerical calculations we will use values of  $s$  and  $\rho$  as given by Wiebes <sup>2)</sup> and by Lounasmaa <sup>3)</sup>,  $\rho_n$  and  $\rho_s = \rho - \rho_n$  can then be obtained from the experimental data on the velocity of second sound under pressure <sup>4)</sup>. However, for the temperature region considered in this section we used the more convenient relation

$$\frac{\rho_n}{\rho} = \frac{s}{s_\lambda}$$

where  $s_\lambda$  is the entropy per gram at the lambda temperature.

In order to find the function  $F_{sn}$  we draw attention to the shape of the curve for  $\dot{Q}_H = 2688 \text{ erg s}^{-1}$  (curve e in fig. 3b), in the vicinity of point A where  $T_a = T_b$ , the bath temperature, and  $v \approx 17 \text{ cm s}^{-1}$ . From a calculation of  $v_n$  from the relation  $\dot{Q}_H = 0_c \rho_s \rho_b T_b v_n$ , where again  $v_n$  is the normal transport velocity, averaged over the cross-section of the capillary, it is found that everywhere in the capillary also  $v_n \approx 17 \text{ cm s}^{-1}$ , so that  $\frac{dT}{dx}$  appears to become zero for  $v_n \approx v_s \approx v$ .

From eq. (6) (or rather from eqs. (3) or (4), but from the direct measurements of the pressure differences by Staas et al.<sup>5)</sup> the terms

$$-\frac{\rho_n}{\rho} \frac{dP}{dx} - F_n = \frac{\rho_s}{\rho} \frac{dP}{dx} + F_s$$

can be expected to be small at these values of the velocities), it follows that  $F_{sn}$  becomes zero for  $v_n \approx v_s \approx v$ . In addition, close to point A the curve shows an inflection point where its first derivative becomes very small, so that it is suggested that  $F_{sn}$  contains a factor  $(v_s - v_n)^3$ . It is therefore tempting to try the well known expression for the mutual friction force  $F_{sn}$ , first suggested by Gorter and Mellink<sup>6)</sup>. They explain the cubic dependence of the temperature gradient on the heat flux and the break-down of the validity of London's equation  $\text{grad } P = \rho_s \text{ grad } T$ <sup>7)</sup> in their experiments on heat conduction in He II at saturated vapour pressure, by introducing

$$F_{sn} = A(T) \rho_s \rho_n (v_s - v_n)^3 \quad (7)$$

The quantity  $A(T)$  was found to be a slowly varying function of temperature in the order of  $50 \text{ cm s g}^{-1}$ .

From the following discussion it will appear that this attempt works out rather successful.

### 3.1.1. *The calculation of A from the curves for which $\dot{Q}_H = 0$*

Let us first turn our attention to the two curves a given for  $\dot{Q}_H = 0$  and  $T_b = 1.455 \text{ K}$  respectively  $1.152 \text{ K}$ . (Figs. 3a and b.) Since  $A(T)$  is as yet undetermined it will always be possible to determine  $A(T)$  as a function of temperature from each of the two curves a individually. By combining eqs. (6) and (7) and by making use of the relation

$$\frac{\rho_n}{\rho} = \frac{s}{s_\lambda} ,$$

one obtains the following expression for the temperature gradient in the capillary

$$\frac{dT}{dx} = \frac{A\rho}{s_\lambda} \left(\frac{\rho}{\rho_s}\right)^3 \left(v - \frac{\dot{Q}_H}{0_c \rho s T}\right)^3 \quad (8)$$

From this equation and from the boundary conditions that  $T = T_a$  at  $x = 0$  and  $T = T_b$  at  $x = \ell$ , with  $\ell$  the length of the capillary, it follows that for  $\dot{Q}_H = 0$

$$\int_{T_a}^{T_b} \frac{1}{A} \left(\frac{\rho_s}{\rho}\right)^3 dT = \int_{T_a}^{T_b} \frac{\rho}{s_\lambda} v^3 \frac{dx}{dT} dT = \frac{\rho}{s_\lambda} v^3 \ell \quad (9)$$

Since we did not measure the temperature locally at  $x = \ell$ , we cannot be completely sure that the helium at  $x = \ell$  is exactly at bath temperature; we have experimental evidence that under certain conditions helium leaving the capillary can be at a temperature considerably different from that of the bath (Ch. III). Nevertheless, in order to pursue our present analysis, we will assume that in the velocity region considered here  $T = T_b$  at  $x = \ell$ . With the help of the experimental relation between  $T_a$  and  $v$  of figs. 3a and b, and the known values of  $\frac{\rho_s}{\rho}$  at a pressure of 10 atm  $A(T)$  can now be determined numerically from eq. (9). Fig. 4 shows the results of  $A(T)$  calculated in this way for both curves where  $\dot{Q}_H = 0$ . It is clear from this figure that in the common temperature region the results for  $A(T)$  are quite different and it seems at first sight that a mutual friction force of the Gorter-Mellink type does not give a satisfactory description of the phenomena. However there is one important phenomenon we have not taken into account yet, i.e., the heat production which takes place in the capillary. On thermodynamical grounds it can be easily shown that the heat flux  $\vec{q}$  obeys the relation

$$\text{div } \vec{q} = -\rho \vec{v} \cdot \vec{\nabla} \mu \quad (10)$$

Since we neglect the pressure difference over the capillary this means that  $\dot{Q}_H$  in equation (8) has to be replaced by

$$\dot{Q}(x) = \dot{Q}_H + 0_c \rho v \int_0^x s \frac{dT}{dx'} dx' = \dot{Q}_H + 0_c \rho v \int_{T_a}^T s dT'$$



Fig. 4.

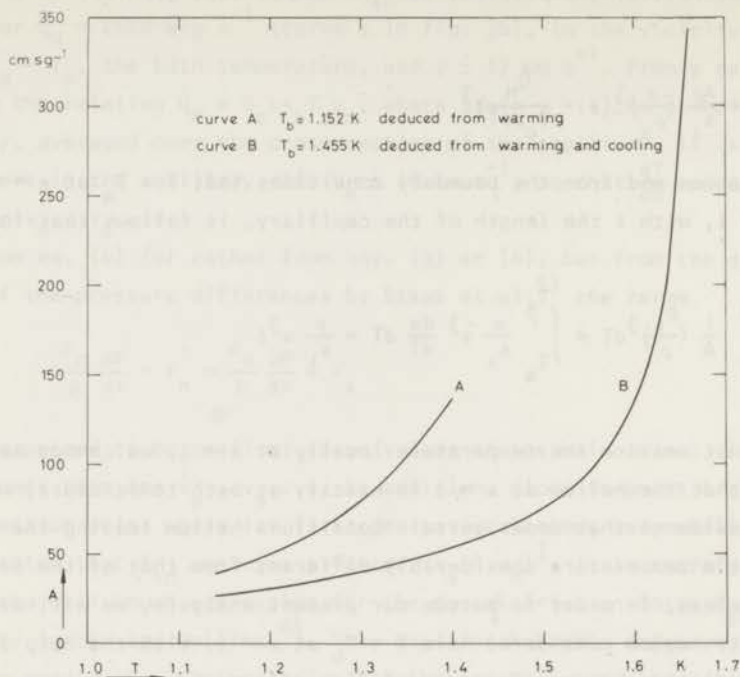
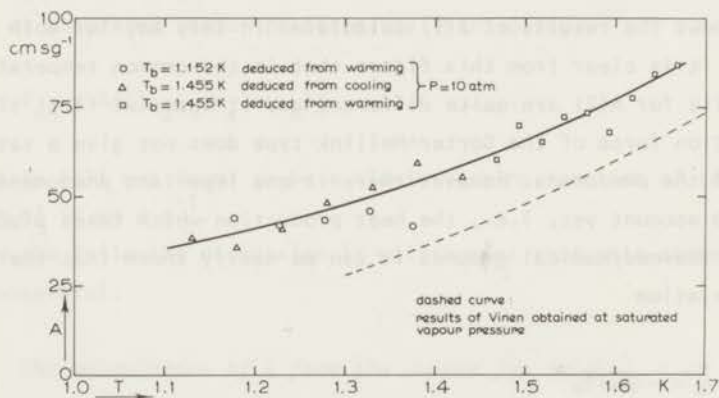


Fig. 5.



Figs. 4 and 5. The mutual friction constant at a pressure of 10 atm as calculated from the curves a in fig. 3a and b. The results shown in fig. 4 are calculated by means of eq. (9) whereas the results of fig. 5 are calculated by means of eq. (11), viz. by taking into account the dissipation. The dashed curve in fig. 5 shows the results of Vinen obtained at saturated vapour pressure.



Equation (8) reads now, when heat production is taken into account,

$$\frac{dT}{dx} = \frac{A\rho}{s_\lambda} \left(\frac{\rho}{\rho_s}\right)^3 v^3 \left[ 1 - \frac{\dot{Q}_H}{0_c \rho_s T v} - \frac{\int_{T_a}^T s dT'}{sT} \right]^3 \quad (11)$$

Again, eq. (11) gives  $\frac{dT}{dx}$  as a known function of temperature apart from the unknown function  $A(T)$ .

Using a similar method as described above, we calculated from eq. (11)  $A(T)$  for both curves with  $\dot{Q}_H = 0$ .

The result of this calculation is shown in fig. 5 where we have plotted calculated values of  $A(T)$  for both series together. The solid curve represents a smooth curve drawn through the calculated points. That both  $T_a$  versus  $v$  curves are well described by this smoothed curve for  $A(T)$  is demonstrated in fig. 6. Now we have reversed the procedure and we have calculated  $T_a$  for  $\dot{Q}_H = 0$  as a function of  $v$  for both bath temperatures, using eq. (11) and the smoothed values of  $A(T)$ . The calculated curves coincide nicely with the measured points, showing that the rather large spread in the computed points in fig. 5 is due to the numerical calculation method. In fig. 5 the dashed curve shows  $A(T)$  determined by Vinen from thermal conduction measurements and from measurements of the attenuation of second sound performed at saturated vapour pressure<sup>8)</sup>.

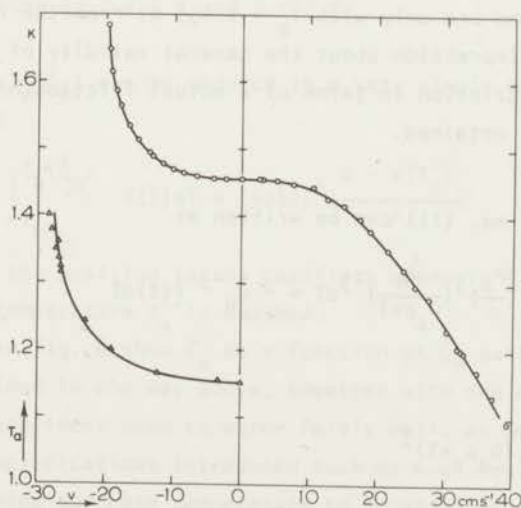


Fig. 6. Comparison between the experimental data points of  $T_a$  as a function of the net mass flow velocity with the calculated curve.

A comparison between the two curves seems to be reassuring, A being somewhat higher at high pressure but with a very similar temperature dependence.

### 3.1.2. The calculation of $T_a$ as a function of $v$ for $\dot{Q}_H \neq 0$

A crucial test for the validity of a description of the flow phenomena in terms of a mutual friction force of the Gorter-Mellink type, is now to calculate the temperature difference  $\Delta T$  over the capillary for any combination of  $\dot{Q}_H$  and  $v$ , using the A values found previously from the experiments with  $\dot{Q}_H = 0$ .

From eq. (11) which can be written as

$$dx = \frac{s_\lambda}{A\rho} \left(\frac{\rho s}{\rho}\right)^3 v^{-3} \left[ 1 - \frac{\dot{Q}_H}{0_c \rho s T v} - \frac{\int_{T_a}^T s dT'}{sT} \right]^{-3} dT \quad (11a)$$

the temperature distribution  $T(x)$  can be obtained by numerical integration for any  $\dot{Q}_H$  and  $v$ , if we assume again that at  $x = \ell$  the helium is exactly at bath temperature. Since the calculation of  $T_a$  for a given combination of  $\dot{Q}_H$  and  $v$  is quite elaborate, we have restricted ourselves to the calculation of  $T_a$  (and thus  $\Delta T$ ) from the experimental values of  $\dot{Q}_H$  and  $v$  obtained at two intersections in figs. 3a and b, namely one at  $v = 0$  and one at the experimental value  $T_a = 1.676$  K, the first one with the bath temperature at 1.152 K as well as 1.455 K, the second one only with  $T_b = 1.455$  K. From the results of these calculations a good impression about the general validity of the present phenomenological description in terms of a mutual friction of the Gorter-Mellink type can be obtained.

3.1.2.a. For  $v = 0$ , eq. (11) can be written as

$$dx = - \frac{s_\lambda}{A\rho} \left(\frac{\rho s}{\rho}\right)^3 \left(\frac{\dot{Q}_H}{0_c \rho s T}\right)^{-3} dT = - \dot{Q}_H^{-3} f(T) dT \quad (12)$$

with

$$f(T) \equiv \frac{s_\lambda}{A\rho} (0_c \rho s T)^3$$

a known function of temperature. In fig. 7 the calculated temperature distributions for  $\dot{Q}_H = 5082$  erg  $s^{-1}$  and  $T_b = 1.455$  K respectively  $T_b = 1.152$  K are shown.

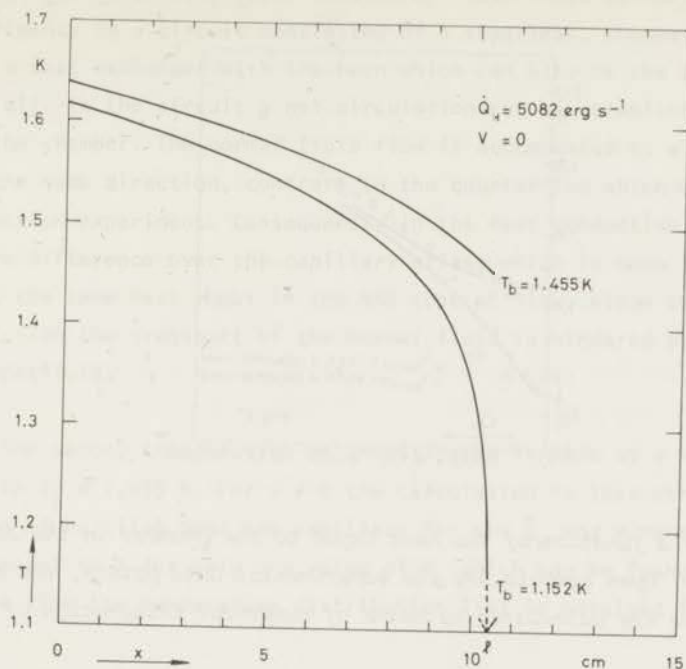


Fig. 7. The calculated temperature distribution along the capillary for  $v = 0$  and a heat input to the chamber of  $5082 \text{ erg s}^{-1}$  at a bath temperature of  $1.455 \text{ K}$  and  $1.152 \text{ K}$ .

From these curves  $T_a(\dot{Q}_H)$  can be deduced in a very simple manner. Integration of eq. (12) yields

$$\dot{Q}_H^3 = \frac{1}{\ell} \int_{T_b}^{T_a(\dot{Q}_H)} f(T) dT = (5082)^3 \left( \frac{\ell - x(T_a)}{\ell} \right) \quad (13)$$

in which  $x(T_a)$  is the position in the capillary where in fig. 7 for  $\dot{Q}_H = 5082 \text{ erg s}^{-1}$  the temperature  $T_a$  is reached.

The solid curves in fig. 8 show  $T_a$  as a function of  $\dot{Q}_H$  calculated for both bath temperatures outlined in the way above, together with the experimental points. Calculation and experiment seem to agree fairly well, as well as can be expected in view of the simplifications introduced such as e.g. neglecting the pressure gradient and assuming the bath temperature to be attained at  $x = \ell$ . The fact that the experimental data points for the bath temperature of  $1.152 \text{ K}$  coincide with those at a bath temperature of  $1.455 \text{ K}$  above a certain value of  $\dot{Q}_H$  is rather unexpected, although the calculated curves do not predict a large

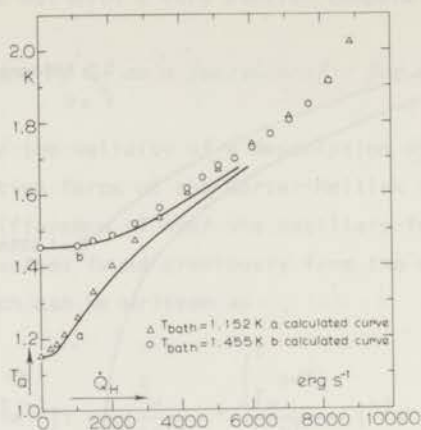


Fig. 8.  $T_a$  as a function of the heat input to the chamber in the case that  $v = 0$ . Open symbols are the experimental data points, the solid curves are calculated by means of numerical integration of eq. (12).

temperature difference between these two cases.

For large heat flows the temperature of the bath thus seems to become irrelevant, which would mean that the temperature at  $x = l$  is the same for both sets of data and probably even higher than 1.455 K. In the present theory and in any theory that considers only stationary flow, the coupling to the bath is effectuated only by the necessity of imposing a boundary condition at  $x = l$ . In view of this remark it is clear that measurements of the temperature at  $x = l$ , or rather the temperature distribution along the capillary are badly wanted. Nevertheless, the rather good agreement between theory and experiment shown in fig. 8 allows us to continue the analysis still by assuming that  $T = T_b$  at  $x = l$ .

It may be of interest to mention that when the valve II (see fig. 2) was opened during a measuring run at  $v = 0$  we observed the temperature difference  $\Delta T$  over the capillary to decrease to a much smaller value. This can be understood qualitatively since, via the gas in the circuit at room temperature, a net circulation of the helium can now be established in the system corresponding to  $v > 0$  and consequently to a smaller  $\Delta T$  (see fig. 3b).

Although we have not analysed these observations in great detail the experimental situation reminds us of a type of flow encountered in experiments carried out by Staas et al.<sup>5)</sup> and by Van der Heijden et al.<sup>9)</sup> who calls this



type of flow non restricted superfluid (NRS) flow. These authors have performed flow experiments in a circuit consisting of a superleak, chamber and capillary closed by a heat exchanger with the bath which can also be the bath itself (Staas et al). In the circuit a net circulation can be established by a heat input to the chamber. The normal fluid flow is accompanied by a flow of superfluid in the same direction, contrary to the counterflow which occurs in a pure heat conduction experiment. Consequently in the heat conduction experiment a temperature difference over the capillary arises which is much larger than that arising at the same heat input in the NRS type of flow, since through the mutual friction the transport of the normal fluid is hindered by the counterflow of superfluid.

3.1.2.b. The second intersection we investigated is made at a value of  $T_a = 1.676$  K with  $T_b = 1.455$  K. For  $v \neq 0$  the calculation is less straightforward. Integration of eq.(11a) over the capillary for any  $\dot{Q}_H$  and  $v$  makes the right hand side equal to  $\lambda$  for only one value of  $T_a$  which can be found by iteration. At the same time the temperature distribution  $T(x)$  is obtained from these calculations.

Fig. 9 shows the calculated temperature distribution along the capillary for three extreme values of  $v$  (the highest values of  $v$  in positive and negative direction and  $v = 0$ ), with the appropriate values of  $\dot{Q}_H$ . For  $T_a$  we find from fig. 9 the values:

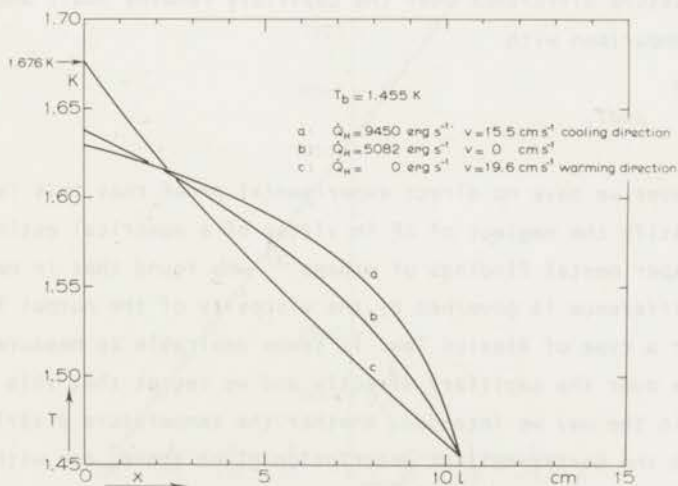


Fig. 9. The calculated temperature distribution along the capillary for three extreme values of  $v$ , at the bath temperature of 1.455 K.



$$T_a = 1.676 \text{ K, for } v = -19.6 \text{ cm s}^{-1} \text{ and } \dot{Q}_H = 0,$$

$$T_a = 1.638 \text{ K, for } v = 0 \text{ and } \dot{Q}_H = 5082 \text{ erg s}^{-1} \text{ and}$$

$$T_a = 1.629 \text{ K, for } v = +15.5 \text{ cm s}^{-1} \text{ and } \dot{Q}_H = 9450 \text{ erg s}^{-1}.$$

In order to show that the results from the calculation are in fair agreement with experiment, it appears unnecessary to carry out the rather elaborate iteration process. We have simply taken  $T_a$  occurring in the brackets of eq. (11a) equal to the experimental value 1.676 K. Of course it is not surprising to see that in the first case the agreement is perfect, since the mutual friction constant was determined from the data with  $\dot{Q}_H = 0$ . In the third case the agreement is fair and could even be somewhat improved by using the iterative process.

Hence also for the intersection at constant temperature the calculations are in satisfactory agreement with the measurements.

From the analysis above we conclude that a two fluid model including mutual friction of the Gorter-Mellink type gives a good description of all results presented in figs. 3a and 3b, obtained for different types of adiabatic flow. In our opinion the discrepancies between the calculations and the measurements do not necessarily imply a shortcoming of the Gorter-Mellink description, but can possibly be accounted for by the simplifying assumption we made using a boundary condition at  $x = l$  ( $T_{x=l} = T_b$ ) and by the total neglect of the pressure difference over the capillary.

In a previous paper we provided experimental evidence that in the case that  $\dot{Q}_H = 0$ , the pressure difference over the capillary remains small and can be neglected in comparison with

$$\int_T^{T+\Delta T} \rho s dT.$$

For  $\dot{Q}_H \neq 0$  however we have no direct experimental proof that this is true and we can only justify the neglect of  $\Delta P$  in virtue of a numerical estimate of  $\Delta P$  based on the experimental findings of others<sup>5)</sup> who found that in many cases the pressure difference is governed by the viscosity of the normal fluid through a Poiseuille or a type of Blasius law. It seems desirable to measure the pressure difference over the capillary directly and we regret that this appeared to be impossible in the way we intended. Whether the temperature distribution, calculated from the Gorter-Mellink description given above, can withstand a confrontation with experiment remains open for investigation.

Finally we would like not to omit the mention of a striking experimental

result shown in fig. 10 which we encountered in the analysis of the intersection at constant temperature difference.

In this figure the values of  $\dot{Q}_H$  and  $v$  which all yield the same temperature of 1.676 K are plotted against each other and apparently a straight line through these data points can be drawn. This is not only the case with the intersection in question but also with intersections at intermediate temperatures between 1.676 K and  $T_b$  while the same is true for the experiments performed at a bath temperature of 1.152 K. One can wonder whether these findings are accidental or that there exists a basic reason for them. Starting from eq. (11) it proves impossible to deduce such linear relationships analytically (though we have shown in the foregoing that the numerical agreement of the data with eq. (11) is quite satisfactory). Furthermore, we believe from the following argument that a linear relationship cannot be basic. Suppose we extrapolate the straight line of fig. 10 to a value of  $\dot{Q}_H$  where the corresponding  $v_n$  at 1.676 K is equal to  $v$ . In this situation the flow should be of the NRS type with  $\Delta\mu$  equal to zero<sup>5,9</sup>). This value of  $v_n = v$  is found to be  $\approx 40 \text{ cm s}^{-1}$ . The pressure difference  $\Delta P$  corresponding to this value of the velocity can be derived from a

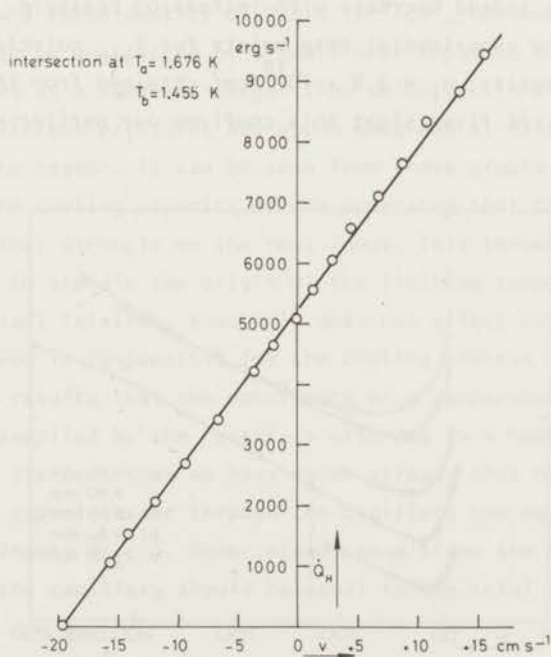


Fig. 10. The heat input to the chamber versus the net mass flow velocity, obtained from the intersection at  $T_a = 1.676 \text{ K}$  in fig. 3b.

type of Blasius law<sup>9)</sup>. It is found to be much too small in comparison with a temperature difference of 0.221 K to obey the equation

$$\Delta P = \int_{1.455\text{K}}^{1.676\text{K}} \rho s dT$$

We therefore conclude that the curve in fig. 10 cannot remain straight but has to bend upwards at higher values of  $\dot{Q}_H$  as to reach the situation  $v_n = v$  at much higher values of  $\dot{Q}_H$ .

### 3.2. Measurements of $T_a$ close to its minimum value

In this section the influence of the overall pressure on the limiting temperature will be investigated. This temperature was expected to decrease with increasing pressure due to the increasing roton density. Fig. 11 shows  $T_a$  as a function of the flow velocity  $v$  in the capillary in the vicinity of the minimum temperature attainable, as measured at five different overall pressures.

As can be clearly seen from this figure and from fig. 12 the minimum temperature,  $T_{\min}$ , does indeed decrease with increasing pressure. It is interesting to note that the experimental data points for  $T_{\min}$  coincide with a curve at constant roton density,  $N_r = 9.8 \times 10^{18}/\text{cm}^3$ , obtained from the data of Wiebes (drawn line). At first sight this confirms our earlier suggestion that

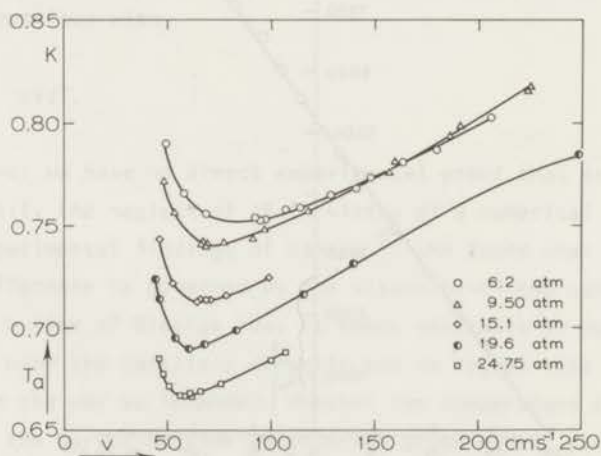


Fig. 11.  $T_a$  near its minimum value as a function of the net mass flow velocity at five different overall pressures.

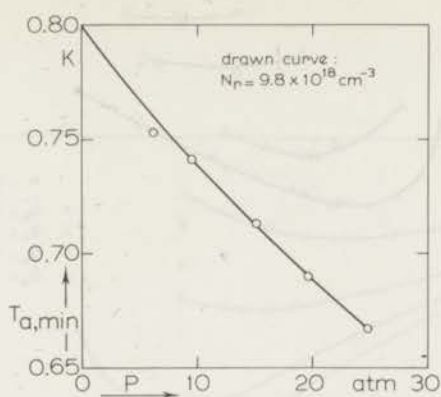


Fig. 12. The measured minimum value of  $T_a$  as a function of the overall pressure.

the roton density plays an important role. If the limitation of the cooling process is indeed due to the fact that the mutual friction force  $F_{sn}$  becomes ineffective below a roton density of  $9.8 \times 10^{18}/\text{cm}^3$ , one would expect the minimum temperature to be unaffected by a small heat input to the chamber; it would merely be attained at a somewhat larger flow velocity. In figures 13a, b, c, d, e results for different pressures are shown obtained at different heat inputs  $\dot{Q}_H$  supplied by the heater. It can be seen from these graphs and also from fig. 14 which shows the cooling capacity of the apparatus that the minimum temperature depends rather strongly on the heat input. This throws considerable doubt upon our attempt to explain the origin of the limiting temperature by the disappearance of mutual friction, though it does not affect our conclusion that the mutual friction is responsible for the cooling process itself. It is rather suggested by the results that the occurrence of a temperature limit in the case that no heat is supplied by the heater is also due to a heat input to the chamber, in spite of the fact that we have shown already that heat leaks from the bath through the superleak nor through the capillary can be responsible for this extra heat input,  $\dot{Q}_{ch}^1$ ). Under steady conditions the heat flow out of the chamber through the capillary should be equal to the total heat input so that

$$0_c \rho_s a T_a v_{n,a} = \dot{Q}_{ch} + \dot{Q}_H \quad (14)$$

where  $0_c$  is the cross-sectional area of the capillary,  $\rho$  the density of helium,



Fig. 13a.

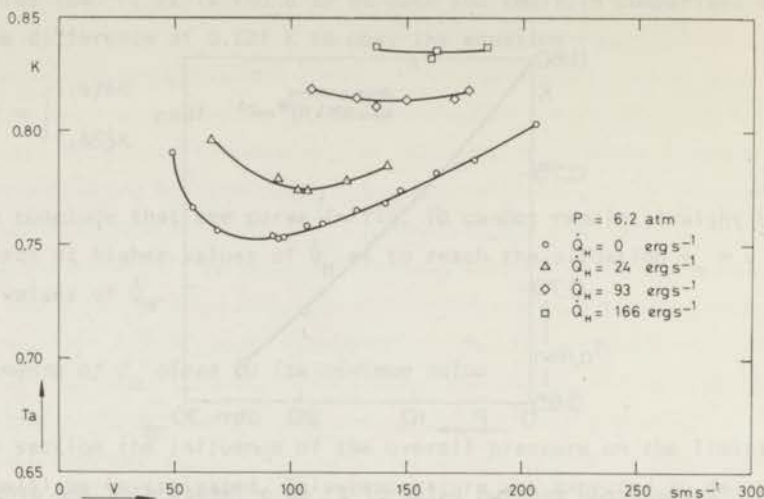


Fig. 13b.

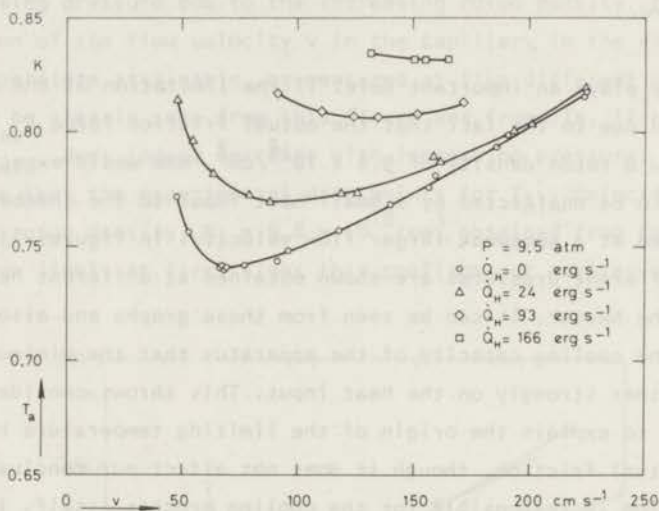


Fig. 13c.

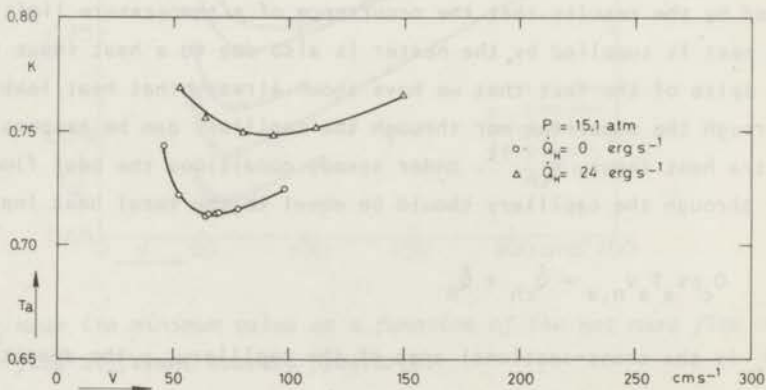




Fig. 13d.

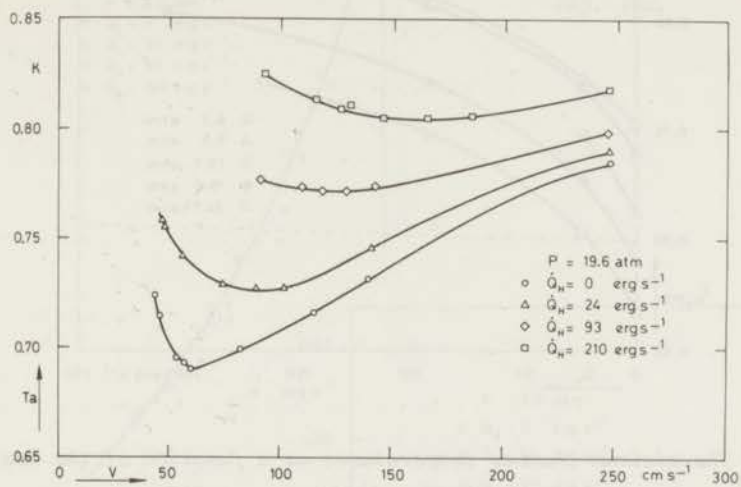


Fig. 13e.

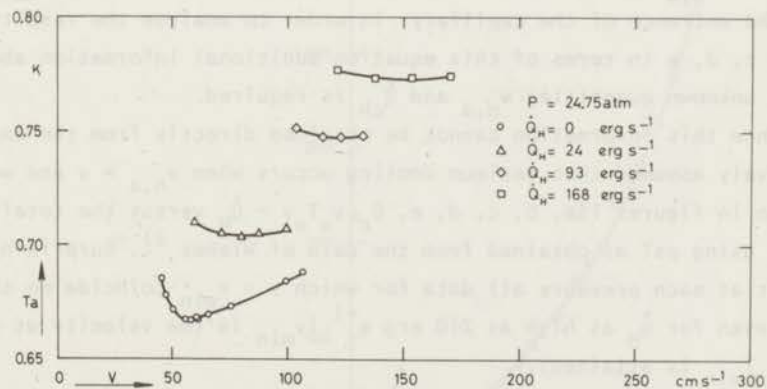


Fig. 13a,b,c,d,e.  $T_a$  as a function of the net mass flow velocity for various heat inputs to the chamber at an overall pressure of 6.2, 9.5, 15.1, 19.6 and 24.75 atm.

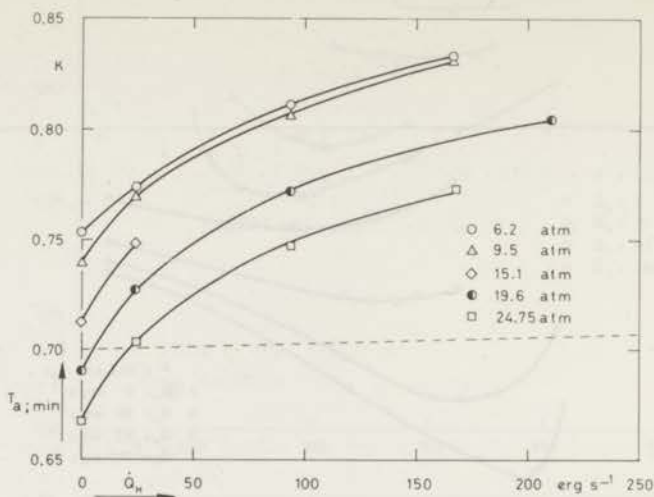


Fig. 14. The minimum chamber temperatures as a function of the heat supplied to the chamber at the five different overall pressures. For comparison the dashed curve shows the cooling capacity of the apparatus of Staas and Severijns (with a 500  $\mu\text{m}$  capillary).

$s_a$ ,  $T_a$  and  $v_{n,a}$  the entropy, temperature respectively normal fluid flow velocity at the entrance of the capillary. In order to analyse the results of figures 13a, b, c, d, e in terms of this equation additional information about one of the two unknown quantities  $v_{n,a}$  and  $\dot{Q}_{ch}$  is required.

Since this information cannot be obtained directly from the experiments we tentatively assumed that maximum cooling occurs when  $v_{n,a} = v$  and we plotted, as shown in figures 15a, b, c, d, e,  $0_c \rho s_a T_a v - \dot{Q}_H$  versus the total flow velocity  $v$ , using  $\rho s T$  as obtained from the data of Wiebes<sup>2)</sup>. Surprisingly it turns out that at each pressure all data for which  $v > v_{min}$  coincide on the same curve, even for  $\dot{Q}_H$  as high as 210 erg s<sup>-1</sup> ( $v_{min}$  is the velocity at which, for  $\dot{Q}_H = 0$ ,  $T_{min}$  is attained).

This result implies that our assumption that  $v_{n,a}$  equals  $v$  leads to the plausible fact that the heat production  $\dot{Q}_{ch}$  is independent of the heat input by means of the heater  $\dot{Q}_H$  and does only depend on the total fluid flow velocity. We reject the possibility that  $v_{n,a} \neq v$  because in that case the heat production has to depend in a rather artificial way on  $\dot{Q}_H$ .

We therefore conclude that heat production in the chamber is responsible for

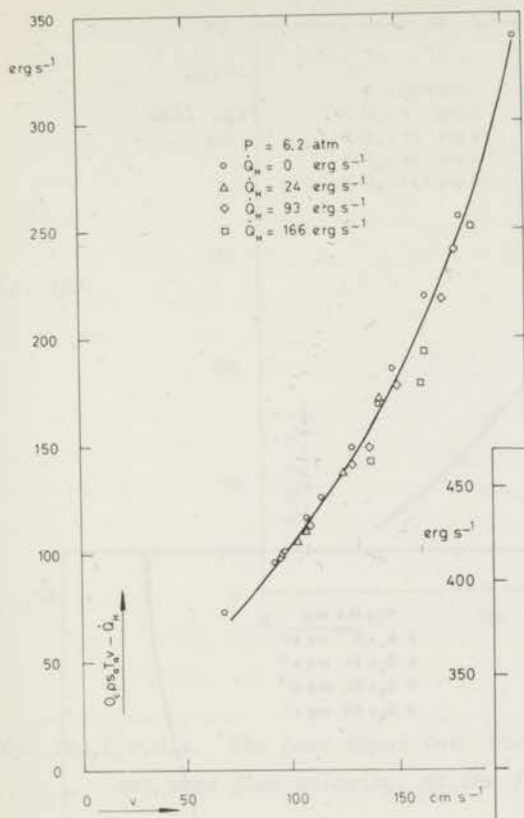


Fig. 15a.

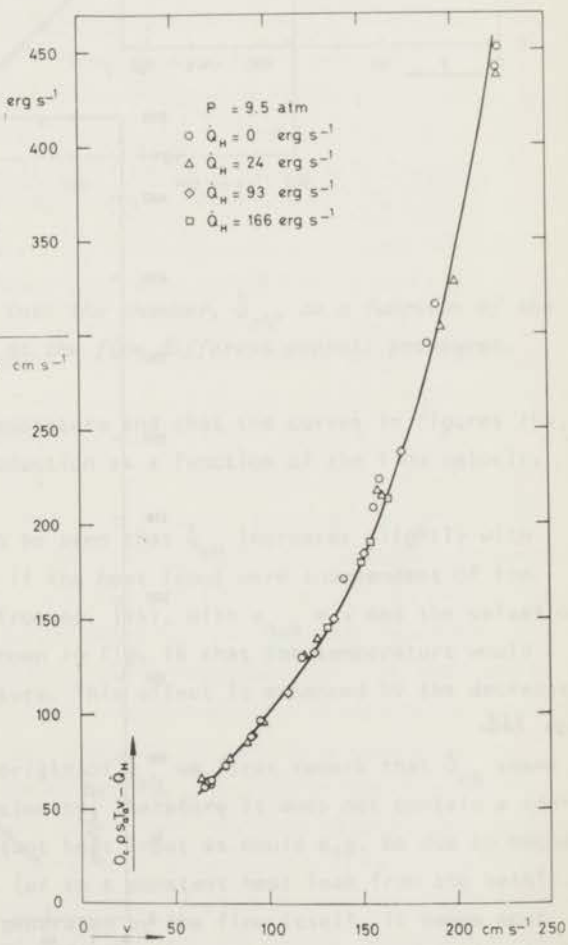


Fig. 15b.

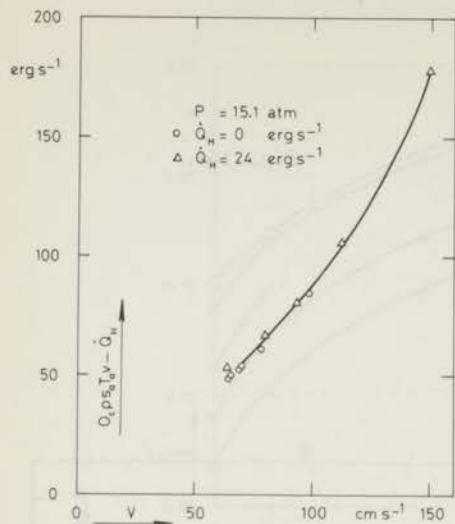


Fig. 15c.

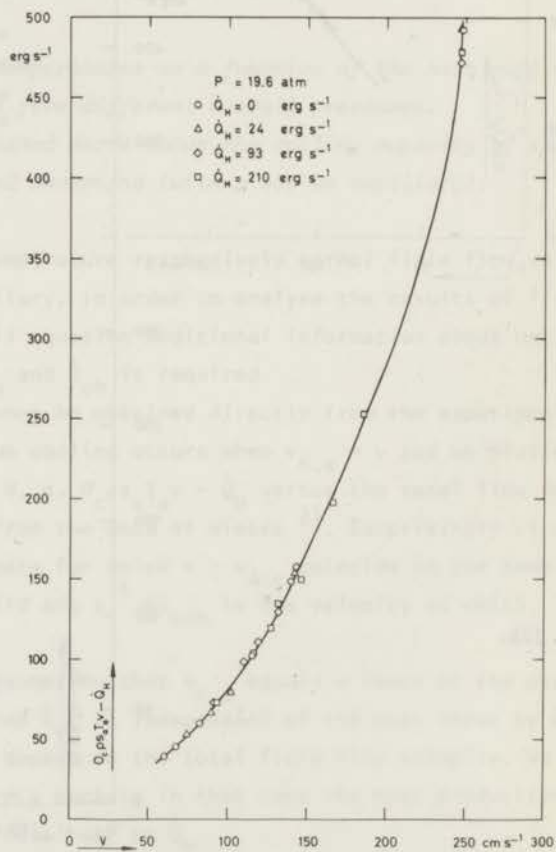


Fig. 15d.



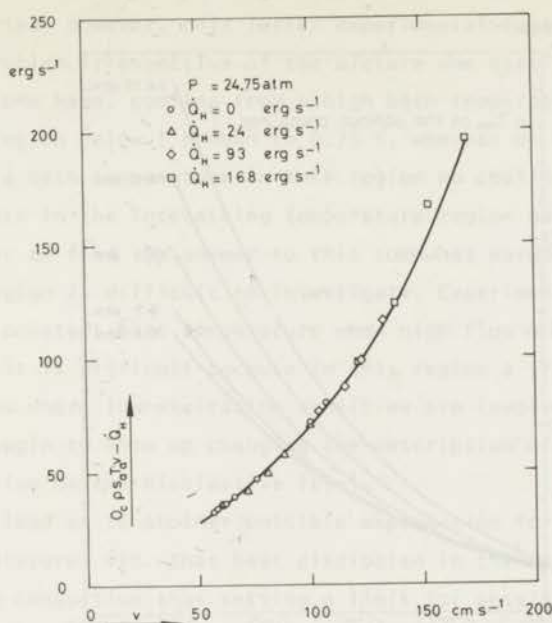


Fig. 15e.

Fig. 15a,b,c,d,e. The heat input into the chamber,  $\dot{Q}_{ch}$ , as a function of the net mass flow velocity, at the five different overall pressures.

the occurrence of the limiting temperature and that the curves in figures 15a, b, c, d, e represent this heat production as a function of the flow velocity  $v$ , for  $v > v_{\min}$ .

From the curves in figs. 15 it can be seen that  $\dot{Q}_{ch}$  increases slightly with increasing overall pressure. Even if the heat input were independent of the overall pressure it would follow from eq. (14), with  $v_{n,a} = v$  and the values of  $\rho s T$  at the various pressures as shown in fig. 16 that the temperature would drop with increasing overall pressure. This effect is enhanced by the decrease of  $\dot{Q}_{ch}$ .

In order to investigate the origin of  $\dot{Q}_{ch}$  we first remark that  $\dot{Q}_{ch}$  seems to extrapolate to zero for zero velocity. Therefore it does not contain a contribution corresponding to a constant heat input as could e.g. be due to mechanical vibrations of the apparatus (or to a constant heat leak from the bath!). From this it follows that  $\dot{Q}_{ch}$  is generated by the flow itself. It seems most likely that dissipation in the chamber itself occurs because a critical velocity

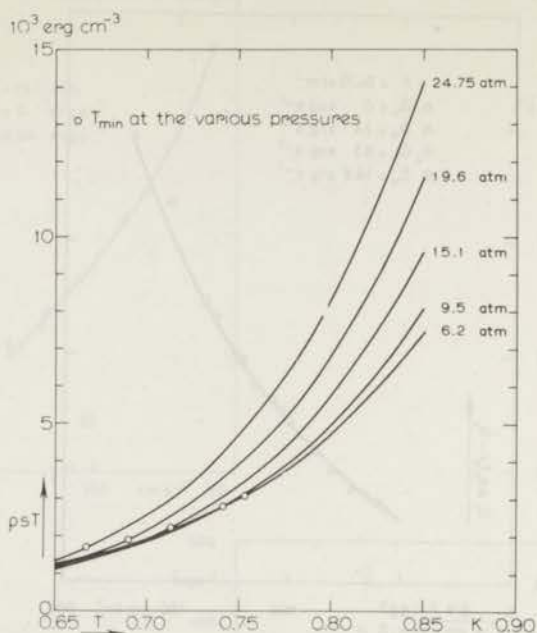


Fig. 16.  $psT$  as a function of temperature at the various pressures used.

is surpassed and a difference in chemical potential over the chamber ( $\Delta\mu_{\text{ch}}$ ) arises so that

$$\dot{Q}_{\text{ch}} = -\rho_0^c v \Delta\mu_{\text{ch}}. \quad (15)$$

(It should be remarked that from an extrapolation of  $\dot{Q}_{\text{ch}}$  down to  $v = 0$  into the region in which  $\dot{Q}_{\text{ch}}$  cannot be obtained directly from experiments, it appears that  $\Delta\mu_{\text{ch}}$  shows the rather peculiar tendency not to become zero at  $v = 0$ ). Although this picture may agree rather well with many experimental findings such as the occurrence of a fixed limiting temperature at nearly equal flow velocities for bath temperatures above 1 K, there are some features which are hardly reconcilable with it. In the vicinity of the minimum in temperature  $\dot{Q}_{\text{ch}}$  is in the order of  $50 \text{ erg s}^{-1}$ , corresponding to a  $\Delta\mu_{\text{ch}}$  of  $\approx 20 \times 10^3 \text{ erg g}^{-1}$  or to a pressure head of 20 cm He. This magnitude of the dissipation is surprisingly high in comparison with the results of Van Alphen et al.<sup>10)</sup>, who found a dissipation at comparable velocities of less than  $1 \text{ erg s}^{-1}$  in their experiments on the energy dissipation in a chamber of similar dimensions enclosed by two superleaks. Furthermore, the picture does not explain the

experimental fact that for bath temperatures between 1 K and 0.75 K no cooling was ever detected. However, this latter experimental fact seems to present a paradoxical problem irrespective of the picture one uses to interpret the results. On the one hand, cooling from a high bath temperature continues "normally" past the region below 1 K down to 0.75 K, whereas on the other hand when starting with a bath temperature in this region no cooling is detected. Careful measurements in the interesting temperature region below 1 K seem to be required in order to find the answer to this somewhat paradoxical problem. This temperature region is difficult to investigate. Experimentally it is difficult to maintain a constant bath temperature when high flow velocities are involved. Theoretically it is difficult because in this region a transition takes place to temperatures where low-excitation densities are involved, so that mean free path effects begin to show up changing the description of the behaviour of superfluid helium on the dissipative level.

These remarks lead us to another possible explanation for the occurrence of a limiting temperature, viz. that heat dissipated in the capillary flows back to the chamber by conduction thus setting a limit for possible cooling. It can be inferred from the calculations by Khalatnikov<sup>11)</sup> that the heat flow due to conduction,  $-0_c KVT$ , is extremely small in comparison to the convective heat flow at temperatures above 1 K. Since most experiments on the flow of He II are carried out at temperatures well above 1 K heat flow by conduction is usually ignored. However at temperatures below 0.8 K this heat flow becomes more and more important. Following this line of reasoning one arrives at the picture that a limit for cooling is reached once the convective heat transport out of the chamber is balanced by the conductive heat flow towards the chamber, i.e.,

$$\rho_s \frac{T}{a} \frac{v}{n_a} = -KVT \quad (16)$$

Although we are aware that also this picture does not fully cover the experimental findings we are inclined to give it an equal chance, provided that eq. (16) turns out to be fulfilled. However, we have no data available on K and on the temperature gradient near the minimum at high overall pressure. In the subsequent chapter in which the measurements on the temperature distributions at "normal" overall pressure will be treated we will come back to this subject.

## References

- 1) Olijhoek, J.F., Hoffer, J.K., Van Beelen, H., De Bruyn Ouboter, R. and Taconis, K.W., *Physica* 64 (1973) 289. Commun. Kamerlingh Onnes Lab., Leiden No. 399b, Chapter 1 of this thesis.
- 2) Wiebes, J., Thesis, University of Leiden (1969).
- 3) Lounasmaa, O.V., *Cryogenics* 1 (1961) 212.
- 4) Maurer, R.D. and Herlin, M.A., *Phys. Rev.* 81 (1951) 444.
- 5) Staas, F.A., Taconis, K.W. and Van Alphen, W.M., *Physica* 27 (1961) 893. Commun. Kamerlingh Onnes Lab., Leiden No. 328d.
- 6) Gorter, C.J. and Mellink, J.H., *Physica* 15 (1949) 285.
- 7) London, H., *Proc. Roy. Soc. London A* 171 (1939) 484.
- 8) Vinen, W.F., *Proc. Roy. Soc. A* 240 (1957) 114.
- 9) Van der Heijden, G., Thesis, University of Leiden (1972).
- 10) Van Alphen, W.M., Olijhoek, J.F., De Bruyn Ouboter, R. and Taconis, K.W., *Physica* 32 (1966) 1901. Commun. Kamerlingh Onnes Lab., Leiden No. 352d.  
Van Alphen, W.M., De Bruyn Ouboter, R., Taconis, K.W. and De Haas, W., *Physica* 40 (1969) 469. Commun. Kamerlingh Onnes Lab., Leiden No. 371a.
- 11) Khalatnikov, I.M., *Zh. éksp. teor. Fiz.* 23 (1952) 8.  
Khalatnikov, I.M. and Chernikova, D.M., *Soviet Phys. JETP* 23 (1966) 274.



## CHAPTER III

### THE TEMPERATURE DISTRIBUTION ALONG THE CAPILLARY DURING STATIONARY FLOW OF He II AT SATURATED VAPOUR PRESSURE

#### *Synopsis*

Extending previous investigations on the cooling effect, the temperature distribution along a thermally isolated capillary through which He II is forced to flow after having passed through a superleak is measured. The temperature gradient at the entrance of the capillary is found to be numerically compatible with the earlier suggestion that heat conduction imposes a limit for cooling. The present results for low velocities appear not to be in agreement with the Gorter-Mellink model. At high velocities the temperature distribution becomes independent of the bath temperature nearly along the entire length of the capillary. From thermodynamics it is shown that the energy dissipated in the capillary is carried away by convective heat transport only, the velocity of the normal component at the end of the capillary being equal to the total mass flow velocity  $v$ .

#### 1. — *Introduction*

In Chapters I and II <sup>1,2)</sup> we described the cooling process which occurs when superfluid helium is forced to flow through a thermally isolated system, formed by a superleak connected in series to a narrow capillary via a small chamber.

In the first chapter we reported on the behaviour of the chamber temperature  $T_a$  as a function of the applied pressure head  $\rho g \Delta Z$ . It was found that a) for small applied pressure heads (i.e., when

$$\rho g \Delta Z < \int_0^{T_b} \rho s dT$$

with  $T_b$  the temperature of the bath prevailing at both ends of the flow system) a cooling of the chamber occurs such that the applied chemical potential difference appears mainly as a temperature difference over the capillary, i.e.,

$$-\Delta\mu = g\Delta Z \approx \int_{T_a}^{T_b} s dT \quad (1)$$

In this region the pressure drop over the capillary can thus be neglected, which implies that the "mutual friction" force  $F_{sn}$  between the superfluid and normal transport can be held responsible for the cooling, i.e.,

$$F_{sn} = -\rho_s \frac{d\mu}{dx} = \rho_s s \frac{dT}{dx} \quad (2)$$

b) for larger applied pressure heads (i.e., when

$$\rho g \Delta Z \geq \int_0^{T_b} \rho s dT$$

a limiting temperature  $T_{min}$  of about 0.75 K is reached, independent of the bath temperature from which the flow starts. It was shown that this limit is not due to heat leaks from the bath and it was suggested that the limiting temperature might be connected to the decreasing roton density, such that at higher overall pressures a lower limiting temperature should be found.

In the second chapter we reported on the behaviour of  $T_a$  as a function of the helium flow velocity  $v$ , at overall pressures ranging from 6 to 25 atm. (See for instance the cooling run at 10 atm in fig. 1).

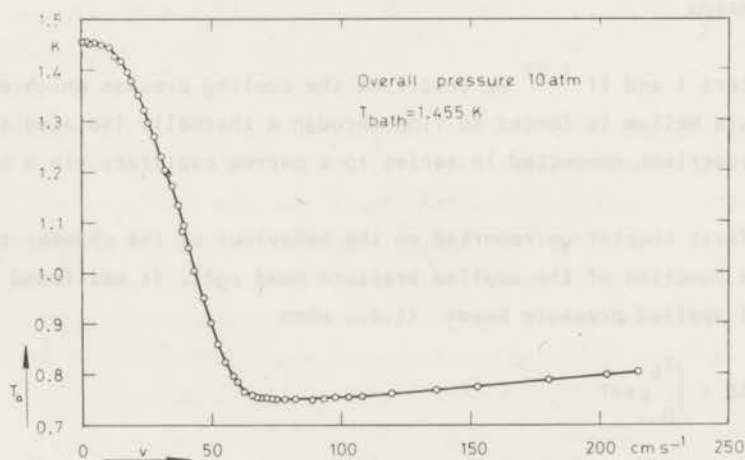


Fig. 1. Example of a cooling run at an overall pressure of 10 atm.

From the whole set of experiments including those on flow in both directions in the presence of a variable amount of heat supplied to the chamber it was a.o. concluded that

c) for small velocities (such that maximum cooling has not yet been reached) the cooling of the chamber can be described by a mutual friction force of the Gorter-Mellink type, i.e.,

$$F_{sn} = A \rho_s \rho_n (v_s - v_n)^3 \quad (3)$$

where  $A$  is found to be slightly temperature dependent. At an overall pressure of 10 atm  $A$  ranges from  $35 \text{ cm sg}^{-1}$  at  $T = 1.1 \text{ K}$  to  $90 \text{ cm sg}^{-1}$  at  $T = 1.7 \text{ K}$ .

d) For large velocities the chamber temperature shows a flat minimum. It was found that  $T_{\min}$  does indeed decrease with increasing overall pressure, such that  $T_{\min}$  occurs at a fixed roton density of about  $10^{19} \text{ cm}^{-3}$ .

It was further found that  $T_{\min}$  increases when heat is supplied to the chamber by the heater mounted against the chamber wall. From these latter measurements it was concluded that

e) the velocity of the normal component,  $v_{n,a}$  at the entrance of the capillary near the chamber, equals the mass flow velocity  $v$  once  $T_{\min}$  is reached.

f) near  $T_{\min}$  heat generated by the flow itself,  $\dot{Q}_{ch}$ , is supplied to the chamber, being in the order of  $50 \text{ erg s}^{-1}$  for the  $208 \text{ } \mu\text{m}$  i.d. capillary used in these experiments. It could not be distinguished whether this heat input is due to the dissipation in the chamber itself, or to dissipation in the capillary, of which the heat produced flows back towards the chamber due to heat conduction  $-K \nabla T$ . (This heat flux at the entrance of the capillary is consequently balanced by the convective heat transport  $\rho_s T_a v_{n,a}$ ).

In the present chapter we will report on measurements of the temperature distributions along the capillary during stationary flow of He II in the analysis whereof the foregoing conclusions will serve as a starting point. These measurements not only seem to be the best way to obtain more information on the flow at high velocities, where  $T_a$  does hardly change anymore, but may also help to solve a number of questions still left open, such as

a) Is the occurrence of a limiting temperature due to heat conduction from the capillary - i.e. is the numerical value of  $K \left[ \frac{dT}{dx} \right]_{x=0}$  comparable with  $\rho(sT)_a v$  - or is it due to dissipation in the chamber itself?

b) Is the temperature at the end of the capillary always equal to the bath temperature? We merely assumed this boundary condition in the analysis of the behaviour of  $T_a$  for different types of flow, given in the previous chapter <sup>2)</sup>

which led to an interpretation in terms of a mutual friction of the Gorter-Mellink type.

c) Is the temperature distribution which would follow from this latter description compatible with experiment?

## 2. Experimental results

Measurements of the temperature distribution along the capillary during stationary flow of helium under normal overall pressure are carried out in the apparatus depicted in fig. 2. Five Allen and Bradley resistance thermometers are mounted at regular intervals along the stainless steel capillary C (100  $\mu\text{m}$  i.d. with a length of 52.5 cm). The large pressure heads which force the liquid through the flow system are obtained in the high pressure head generator <sup>1)</sup>, a thermally isolated glass reservoir in which helium is heated under its own vapour pressure and which is connected to the entrance of the superleak via a wide capillary C' (500  $\mu\text{m}$  i.d. with a length of 10 cm) and a heat exchanging bellows B. For the flow system superleak - chamber - capillary -, the chemical

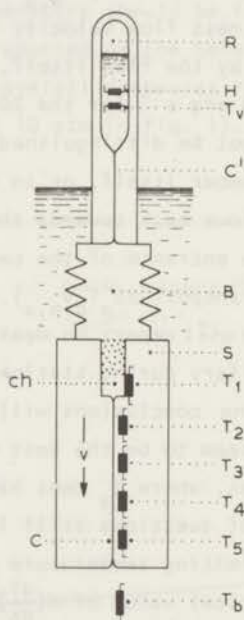


Fig. 2. Schematic diagram of the apparatus.

(R) reservoir, (C') capillary, (B) bellows, (S) superleak, (Ch) chamber, (C) capillary, (H) heater, (T...) thermometer.



potential difference  $\Delta\mu$ , apart from a factor  $\rho$  is equal to the pressure difference, as the low Kapitza resistance of the bellows prevents the occurrence of a temperature difference. Since the pressure drop over the capillary C' can be neglected, this pressure difference over the flow system, for convenience written as  $\rho g \Delta Z$ , is equal to the difference in vapour pressure between reservoir and bath, corrected for the hydrostatic pressure difference. By monitoring the level height in the reservoir the mass flow velocity  $v$  can be obtained.

In fig. 3, the chemical potential difference over the flow system is shown as a function of the flow velocity  $v$  in the capillary for runs at two different bath temperatures. We like to draw attention to the rather abrupt increase in velocity, which appears to occur when the lambda temperature in the reservoir of the high pressure head generator is surpassed. At first sight this apparent increase in  $v$  seems to be due to a sudden decrease in the density of the helium in the reservoir (caused by the formation of vapour bubbles near the heater). However, we also used another high pressure head generator, in so far different from the present one that a longer and wider capillary C' was used (length 22 cm with an inner diameter of 1 mm). Not only the abrupt apparent increase in  $v$

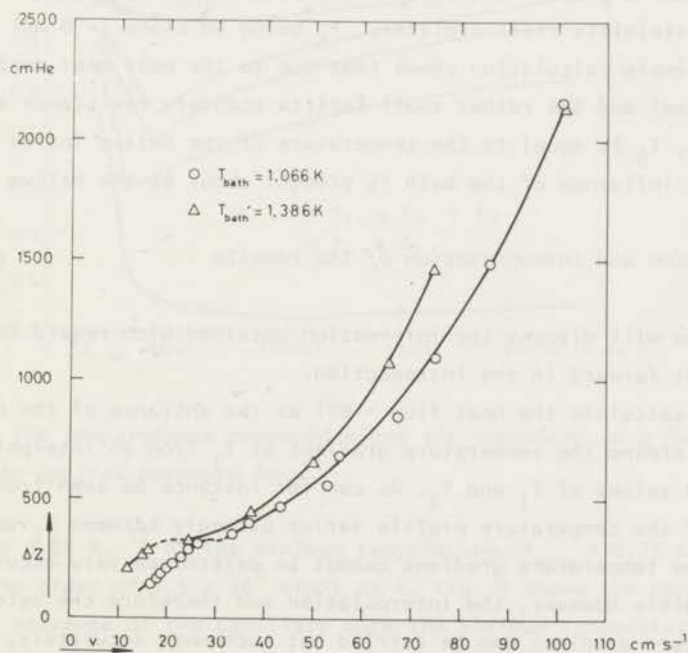


Fig. 3. The applied chemical potential difference over the flow system expressed in cm He as a function of the flow velocity  $v$  in the capillary.

appeared to be much larger, but the simultaneously observed abrupt change of the temperature distribution along the capillary shows that the velocity in the capillary does indeed increase steeply at this point. Therefore, in our opinion, the kink in the  $-\Delta\mu \leftrightarrow v$  curves is only partly due to the decrease in density in the reservoir. It mainly reflects the fact that in general  $\Delta\mu$  over part of a flow system does not determine the flow velocity uniquely but that  $v$  is determined by the flow system as a whole. We will therefore assume that the results shown in fig. 3 are reliable apart from a small, but unknown correction in  $v$  due to the decrease in density in the reservoir.

A survey of the results on the temperature distribution is given in figs. 4 and 5 in which the temperature of the five thermometers is shown as a function of the applied pressure head. It can immediately be seen from these figures that for pressure heads above 500 cm He the temperature distribution becomes rather insensitive for the bath temperature. The influence of the bath mainly shows up in the different behaviour of  $T_5$  at intermediate (500 - 1500 cm) pressure heads,  $T_5$  for a bath temperature of 1.066 K, though higher than that bath temperature, being smaller than  $T_5$  for a bath temperature of 1.386 K. At first sight one might think that this is caused by heat conduction through the wall of the stainless steel capillary,  $T_5$  being so close ( $\approx 8$  mm) to the bath. However, a simple calculation shows that due to the poor heat conduction of stainless steel and the rather small Kapitza boundary resistance at these temperatures,  $T_5$  is equal to the temperature of the helium inside the capillary and that the influence of the bath is brought about by the helium itself.

### 3. *Discussion and interpretation of the results*

First we will discuss the information obtained with regard to the three questions put forward in the introduction.

In order to calculate the heat flux  $-KVT$  at the entrance of the capillary one needs to determine the temperature gradient at  $T_1$  from an interpolation between the measured values of  $T_1$  and  $T_2$ . As can for instance be seen from fig. 6 the curvature of the temperature profile varies strongly between  $T_1$  and  $T_2$  and therefore the temperature gradient cannot be determined very accurately in this way. Fortunately however, the interpolation and therefore the determination of the temperature gradient can be carried out much more accurately, as the quantity  $\rho sT$  appears to increase linearly along nearly the entire length of the capillary (see fig. 7 and 8). A rough estimate of  $K$  can be made from an extrapolation of our data on  $K$  obtained in a similar capillary at temperatures

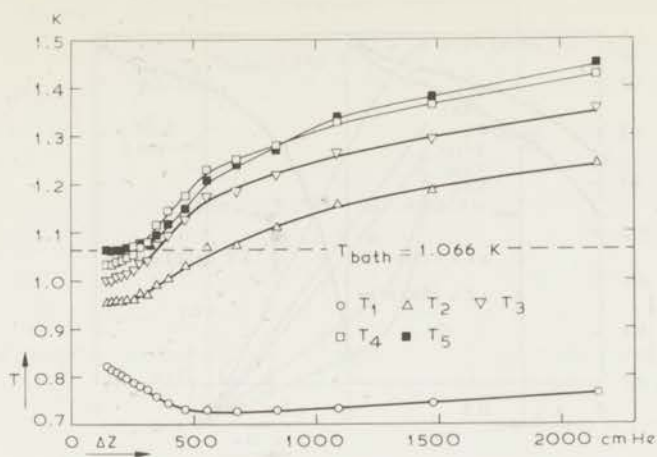


Fig. 4.

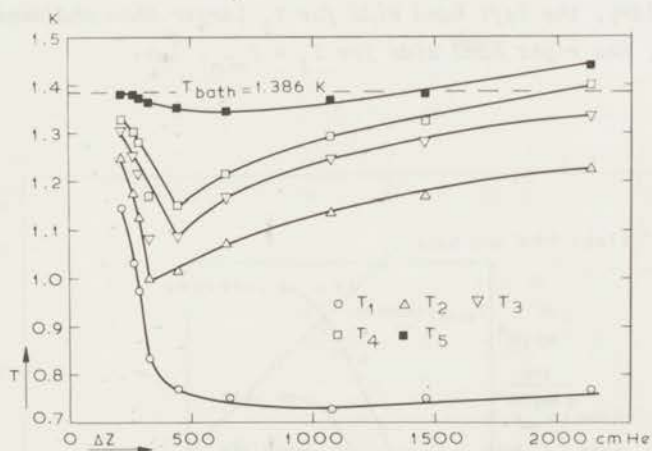


Fig. 5.

Fig. 4 and 5. The temperatures measured along the capillary as a function of the applied pressure head.

between 0.5 and 0.65 K. 1) At the minimum temperature,  $T_{\min} \approx 0.75$  K, one finds that  $K$  is in the order of  $1.5 \times 10^6$  erg/s cm K. Fig. 9 shows the heat flux balance at the entrance of the capillary once the minimum temperature is reached. From this figure it can be seen that the convective heat flux out of the chamber  $\rho s T v$  (where we have used our earlier finding that  $v_n$  equals  $v$  at the minimum 2)) is indeed comparable with the heat flux back to the chamber

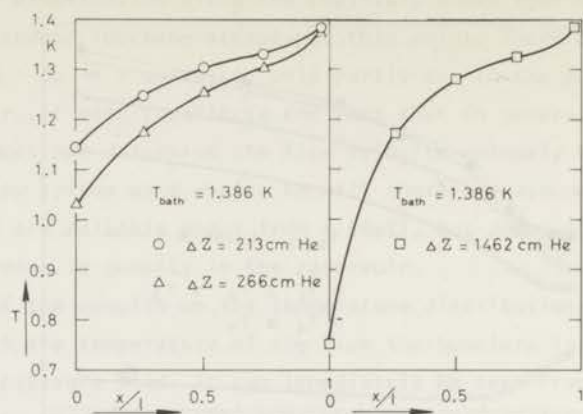


Fig. 6. Example of the measured temperature distribution along the capillary, the left hand side for  $T_1$  larger than the minimum temperature, the right hand side for  $T_1 \approx T_{\text{min}}$ .

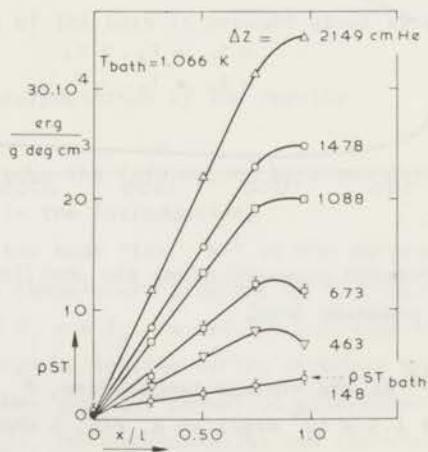


Fig. 7.



Fig. 8.

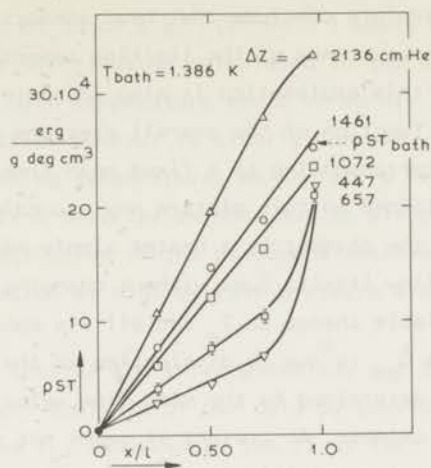


Fig. 7 and 8. The quantity  $\rho s T$  as a function of the position in the capillary.

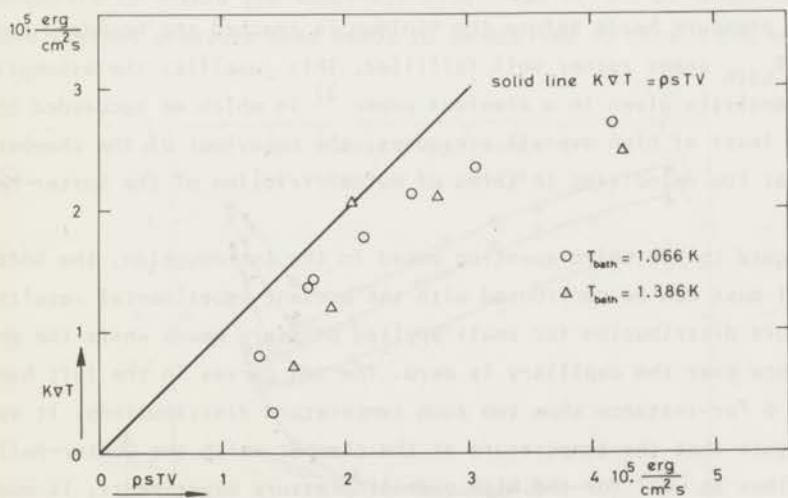


Fig. 9. The heat flux balance at the entrance of the capillary.

due to conduction -  $KVT$ , which in this temperature region can mainly be attributed to phonons.<sup>3)</sup> We therefore conclude that heat conduction provides a possible explanation for the occurrence of the limiting temperature the more so as an indication pointing to this explanation is also found in the fact that the limiting temperature as a function of the overall pressure appears to occur at a fixed roton density corresponding to a fixed mean free path for the phonons. However, it remains unexplained in this picture why according to our earlier findings heat supplied to the chamber by a heater simply adds to the heat input -  $\dot{Q}_{ch}$  - generated by the flow itself, i.e., without changing the magnitude of  $\dot{Q}_{ch}$  in spite of an appreciable change in  $T_a$  and all its consequences. This finding rather indicates that  $\dot{Q}_{ch}$  is due to dissipation in the chamber itself, which should then only be determined by the mass flow velocity  $v$ , independent of the temperature of the chamber. At present it seems not possible to decide unambiguously between these two possible explanations for the occurrence of a limiting temperature.

From figs. 4 and 5 it is immediately clear that the answer to the second question put forward in the introduction has to be in the negative. Especially for high pressure heads and the lower bath temperature the temperature of the helium leaving the capillary is considerably different from that of the bath. We will postpone a discussion of this behaviour for a while and first remark that for low pressure heads before the minimum is reached the boundary condition  $T_{x=l} = T_{bath}$  seems rather well fulfilled. This justifies the assumption made in the analysis given in a previous paper<sup>2)</sup> in which we succeeded to describe, at least at high overall pressures, the behaviour of the chamber temperature at low velocities in terms of mutual friction of the Gorter-Mellink type.

With regard to the third question posed in the introduction, the Gorter-Mellink model must now be confronted with the present experimental results on the temperature distribution for small applied pressure heads where the pressure difference over the capillary is zero. The two curves in the left hand side of fig. 6 for instance show two such temperature distributions. It appears from this figure that the temperature at the chamber which the Gorter-Mellink model<sup>†</sup> describes so well for the high overall pressure experiments, is much

---


$$+ \text{ i.e. } \frac{dT}{dx} = \frac{A\rho}{s_\lambda} \left(\frac{\rho}{\rho_s}\right)^3 \left[1 - \frac{\int_{T_a}^T s dT'}{sT}\right] 3v^3 \quad 2)$$

too low here to be described in this way. Averaged values of  $A$  in the order of  $300 \text{ cm s g}^{-1}$  instead of  $30 \text{ cm s g}^{-1}$  (Vinen <sup>4</sup>) would be required. Even worse is that the temperature distribution calculated in the Gorter-Mellink model with  $A$  slowly increasing with temperature would be mainly convex. The measured temperature distribution however is clearly concave which would require  $A$  to decrease with increasing temperature. We therefore reluctantly have to conclude that the Gorter-Mellink description does not in all circumstances give a good phenomenological description of the phenomena observed. Measurements on the temperature distribution at high overall pressure are in progress.

Having treated thus far the three questions put forward in the introduction we continue the present analysis of our data by considering a plot of the temperatures  $T_1$ ,  $T_2$ ,  $T_3$  and  $T_4$ , measured by the first four thermometers, as a function of the mass flow velocity  $v$  at the two bath temperatures (fig. 10). It is clear from this figure that once the minimum temperature has been reached the temperature distribution in this part of the capillary becomes identical for both bath temperatures. Only in  $T_5$ , the temperature near the exit of the capillary the influence of the bath shows up. That at any given velocity the temperature distribution in the capillary is independent of the temperature of the helium before it enters the superleak (i.e. that of the bellows) seems obvious: only a different pressure head needs to be applied to obtain the same velocity.

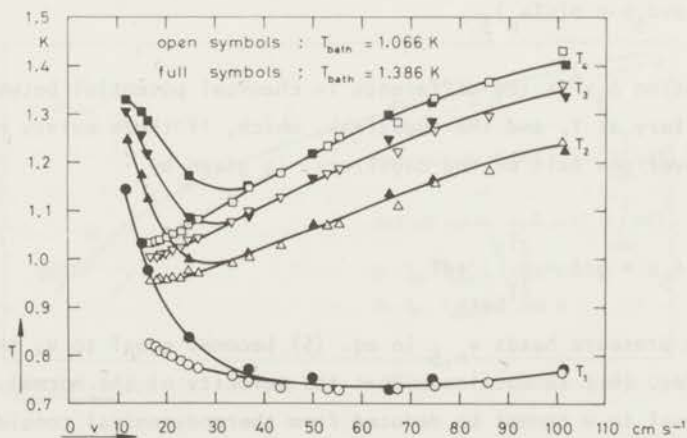


Fig. 10. The first four temperatures measured along the capillary plotted as a function of the flow velocity for the two bath temperatures together.

However that the temperature distribution becomes largely independent of the temperature of the bath at the exit of the capillary is less obvious. For low velocities the bath temperature imposes a boundary condition on the temperature distribution (e.g. for  $v = 0$ ,  $T_{x=l} = T_{\text{bath}}$ ) leading to the difference in temperature profile for the two bath temperatures. However, once the minimum temperature is reached another boundary condition,  $T_1 = T_{\text{min}}$ , is imposed, which at a given velocity leads indeed to identical temperature distributions. The influence of the bath is restricted to only a small portion near the exit of the capillary.

Before commenting on the shape of the experimentally found temperature distributions we will first pay attention to the behaviour of  $T_5$ . For this purpose we draw attention to fig. 11 in which  $T_5$  as a function of the applied pressure head (expressed in cm He) is shown. As can be seen from this figure, the experimental data points for high pressure heads appear to obey the simple relation

$$g\Delta Z = sT - \int_{T_{\text{bath}}}^T s dT' \quad (4)$$

represented by the drawn curves for both bath temperatures. This result is consistent with the idea that the loss of potential energy in the flow system is carried away to the bath by convective heat transport only, i.e.,

$$- \rho v \Delta_5 \mu = \rho (sT_v)_5 \quad (5)$$

In this equation  $\Delta_5 \mu$  is the difference in chemical potential between the end of the capillary at  $T_5$  and the superleak, which, if there exists no pressure difference over the exit of the capillary, is given by

$$- \Delta_5 \mu = g\Delta Z + \int_{T_{\text{bath}}}^{T_5} s dT \quad (6)$$

If, at large pressure heads  $v_{n,5}$  in eq. (5) becomes equal to  $v$ , the experimental result (eq. (4)) is obtained. That the velocity of the normal fluid tends to become equal to  $v$  cannot be deduced from thermodynamical considerations only, but should follow from the hydrodynamics of He II. However, should it indeed follow from hydrodynamics that  $v_n$  cannot be larger than  $v$ , then it is immediately clear that for



$$\Delta Z > \frac{(sT)_{\text{bath}}}{g}$$

the temperature at the end of the capillary will rise above that of the bath. Consequently  $-\Delta_5\mu$  is then larger than the applied chemical potential difference  $g\Delta Z$ . Fig. 11 shows that for smaller pressure heads

$$(\Delta Z < \frac{(sT)_{\text{bath}}}{g}) \quad ,$$

eq. (4) is no longer obeyed (meaning that  $v_{n,5}$  remains smaller than  $v$ ) as the temperature  $T_5$  tends to remain close to the bath temperature in this region.

We like to remark that the fact that the experimental results are consistent with the idea that all energy dissipated in the flow system is accounted for by the heat transported out of the capillary renders support to the calculations of Campbell <sup>5)</sup> who showed that in stationary flow there is no energy available for the creation of vortices.

We conclude that the behaviour of  $T_5$  is understood once it can be shown that  $v_n$  tends to become equal to  $v$  at the end of the capillary as soon as this does no longer imply that the helium leaves the capillary at a temperature lower than the bath temperature. So the ratio  $\frac{v_n}{v}$  (see eq. (5)), and not  $v$  itself determines the temperature at the end of the capillary by the thermodynamical relation (5).

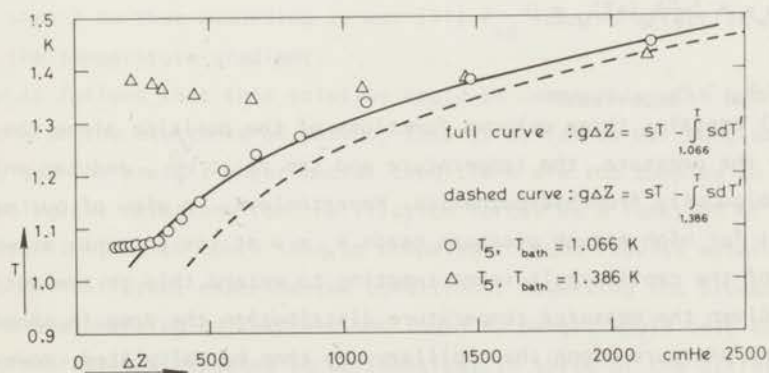


Fig. 11. The temperature at the end of the capillary as a function of the applied pressure head. The open symbols are the measured data points, the curves represent eq. (4).

This latter relation can be shown to apply to every position in the capillary. Let us apply the first law of thermodynamics to a small volume element flowing with the mass flow velocity  $v$ . The rate at which work is done on this element by the pressure is equal to the rate of increase of the internal energy added to the rate at which heat flows out of this element, or

$$-v \frac{dP}{dx} = \rho v \frac{du}{dx} + \frac{d}{dx} [\rho s T (v_n - v) - K \frac{dT}{dx}] \quad (7)$$

where  $u$  is the internal energy per gram and where it is assumed that all kinetic contributions can be neglected, that no heat flows out or into the element through the walls of the flow system and that  $v$  is small compared to the velocity of sound in He II. Implicit use is made of our earlier finding supported by the work of Campbell that no energy is transported by the system of vortices. Integration of this equation yields

$$\rho v \mu + \rho v_n s T - K \frac{dT}{dx} = \text{Constant} \quad (8)$$

where we have made use of the relation  $\mu = u - Ts + \frac{P}{\rho}$ . The value of the constant can easily be found to be  $\rho v \mu_{\text{superleak}}$  by applying eq. (8) to a point in the chamber just behind the superleak. For those points of the flow system where the heat conduction  $-K \nabla T$  can be neglected, say for  $T > 0.8 \text{ K}$ <sup>3)</sup>, eq. (5) is recovered as

$$\Delta_x \mu + \left(\frac{v_n}{v}\right)_x (sT)_x = 0 \quad (9)$$

where  $\Delta_x \mu = \mu_x - \mu_{\text{superleak}}$ .

Equation (9) contains three unknown functions of the position along the capillary namely the pressure, the temperature and the ratio  $\frac{v_n}{v}$ , and can only be solved unambiguously from hydrodynamics. Nevertheless, in view of our earlier finding that for high enough pressure heads  $v_n = v$  at the entrance as well as at the end of the capillary it seems tempting to extend this to the entire capillary. Given the measured temperature distribution the drop in chemical potential and pressure along the capillary can then be calculated. However, the question arises whether this assumption leads to results compatible with hydrodynamics. To begin with, are they compatible with the equations of motion? In the previous chapter<sup>2)</sup> we have written these equations for stationary flow as

$$-\frac{\rho_s}{\rho} \frac{dP}{dx} + \rho_s s \frac{dT}{dx} - F_{sn} - F_s = 0 \quad (10)$$

$$-\frac{\rho_n}{\rho} \frac{dP}{dx} - \rho_s s \frac{dT}{dx} + F_{sn} - F_n = 0 \quad (11)$$

It seems plausible that, whatever being the correct expression for the mutual friction force  $F_{sn}$ , it should contain a factor  $(v_s - v_n)$ . The assumption  $v_n = v$  along the whole capillary thus leads to  $F_{sn} = 0$ . From eq. (11) it then follows that even when  $F_n$  can be neglected this would require pressure heads much higher than those applied. We therefore reject at least as long as we do not question the validity of the equations of motion in the high velocity region the solution  $\frac{v_n}{v} = 1$  along the entire capillary, the more so as for some distributions it turns out from the calculation that near the end of the capillary the pressure gradient would become positive. A more reasonable attempt to solve eq. (9) seems to assume, instead of  $\frac{v_n}{v}$  to be constant, a constant pressure gradient along the capillary given by  $-\frac{dP}{dx} = \frac{\rho g \Delta Z}{l}$ . From the measured temperature distribution together with our finding that at the entrance of the capillary  $\frac{v_n}{v} = 1$  once the minimum is reached one can now calculate  $\Delta_x \mu$  and  $\frac{v_n}{v}$  along the entire length of the capillary. Some results of this calculation are shown in figs. 12 and 13. The following features of these results render support to the validity of the present solution. Fig. 12 shows a nearly constant gradient of the chemical potential, corresponding to a homogeneous dissipation. More important however is the fact that, as appears from fig. 13,  $\frac{v_n}{v}$  is appreciably smaller than 1 so that according to eq. (11)  $F_{sn}$  remains effective in maintaining the temperature gradient.

Herefrom it follows that this solution could be compatible with hydrodynamics, at least with the equations of motion. This is as far as our conclusions can possibly go. The present experimental conditions are too complex to obtain phenomenological relations for the friction forces as a function of the transport velocities, which could then be compared to such results obtained by others under different experimental conditions. Reversing the procedure, i.e., using the phenomenological expressions found by others would only be worthwhile if these expressions happened to be identical in spite of the different experimental conditions under which they were found. It may not be surprising that this appears not to be the case. Fig. 14, for instance, shows some phenomenological relations for the pressure drop over the capillary

$$\Delta P_c = - \int_0^l (F_s + F_n) dx$$

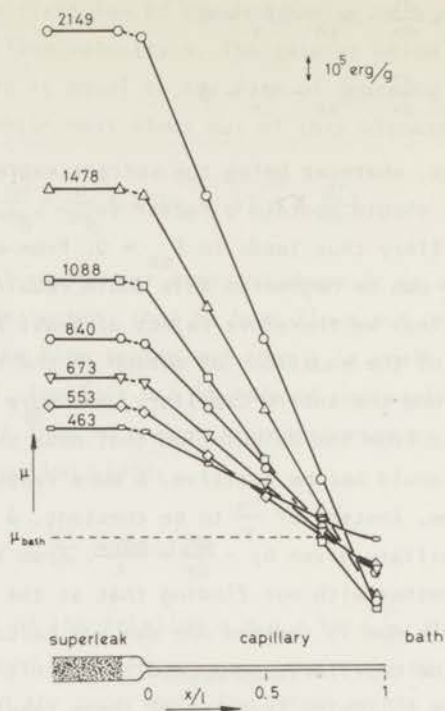


Fig. 12. The drop of the chemical potential along the capillary if a constant pressure gradient is assumed. Numbers represent the applied pressure head (cm He).

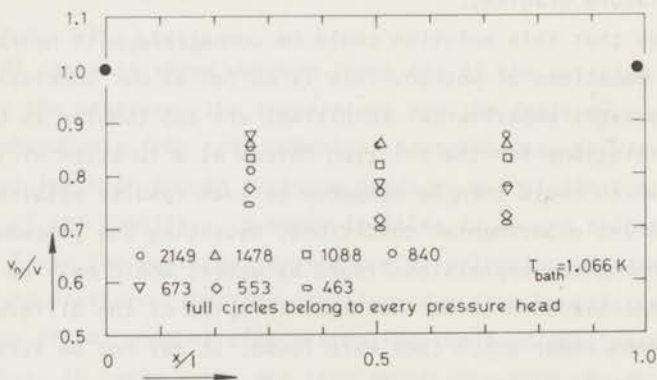


Fig. 13. The ratio  $\frac{v_n}{v}$  along the capillary if a constant pressure gradient is assumed. Numbers correspond to the applied pressure head (cm He).



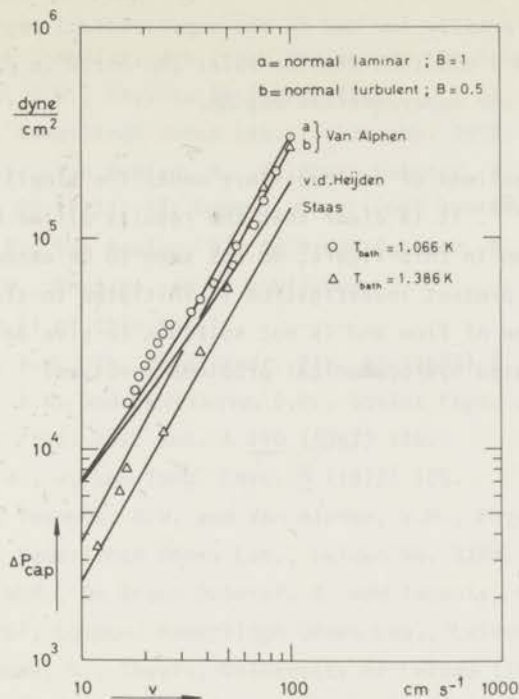


Fig. 14. The pressure drop over the capillary as a function of the flow velocity.

Open symbols are the data points obtained in the present work.

The curves represent the relations according to the work of Staas et al., Van Alphen et al. and Van der Heijden et al.

Staas et al. According to a modified Blasius rule the pressure drop over the capillary is equal to  $0.82 v^{1.75} l$ .

Van Alphen et al. The pressure drop over the capillary is equal to the sum of dissipative and drain pressure. The dissipative pressure is given by  $\Delta P_{diss} = \frac{1}{2} B v^2 l$ , whereas the drain pressure follows either from a Poiseuille rule (laminar flow) or a modified Blasius rule (turbulent flow).

Curve a follows from a dissipative constant  $B = 1 \text{ g cm}^{-4}$  and laminar flow, whereas curve b is calculated for  $B = 0.5 \text{ g cm}^{-4}$  and turbulent flow.

Van der Heijden et al. According to the experiments of these authors the pressure drop corresponding with the flow of normal fluid is always governed by a Poiseuille rule. The flow of superfluid yields

a pressure drop which in the subcritical region ( $\Delta\mu = 0$ ) is governed by a Poiseuille law and in the supercritical region ( $\Delta\mu \neq 0$ ) follows from a modified Blasius rule. The curve in fig. 14 is calculated for the supercritical region.

as applied to the dimensions of our capillary under the simplifying assumption that  $v_n$  equals  $v_s$ <sup>6,7,8</sup>). It is clear that the results differ widely and thus our results, also shown in this figure, do not seem to be exceptional. We like to emphasize that the present investigation is initiated to study the cooling properties of this type of flow and is not suitable to give detailed information on the complicated hydrodynamical problems involved.



## References

- 1) Olijhoek, J.F., Hoffer, J.K., Van Beelen, H., De Bruyn Ouboter, R. and Taconis, K.W., *Physica* 64 (1973) 289;  
Commun. Kamerlingh Onnes Lab., Leiden No. 399b.
- 2) Olijhoek, J.F., Van Beelen, H., De Bruyn Ouboter, R. and Taconis, K.W., *Physica* 69 (1973) 38; Commun. Kamerlingh Onnes Lab., Leiden No. 403b.  
Olijhoek, J.F., Van Beelen, H., De Bruyn Ouboter, R., Taconis, K.W. and Koops, W., *Physica*, to be published.  
Chapter II of this thesis.
- 3) Khalatnikov, I.M., *Zh. éksp. teor. Fiz.* 23 (1952) 8.  
Khalatnikov, I.M. and Chernikova, D.M., *Soviet Phys. JETP* 23 (1966) 274.
- 4) Vinen, W.F., *Proc. Roy. Soc. A* 240 (1957) 114.
- 5) Campbell, L.J., *J. Low Temp. Phys.* 8 (1972) 105.
- 6) Staas, F.A., Taconis, K.W. and Van Alphen, W.M., *Physica* 27 (1961) 893;  
Commun. Kamerlingh Onnes Lab., Leiden No. 328d.
- 7) Van Alphen, W.M., De Bruyn Ouboter, R. and Taconis, K.W., *Physica* 44 (1969) 51; Commun. Kamerlingh Onnes Lab., Leiden, No. 371a.
- 8) Van der Heijden, G., Thesis, University of Leiden (1972).  
*Physica* 59 (1972) 473; Commun. Kamerlingh Onnes Lab., Leiden No. 328d.  
Van der Heijden, G., De Voogt, W.J.P. and Kramers, H.C., *Physica* 59 (1972) 473; Commun. Kamerlingh Onnes Lab., Leiden No. 328d.  
Van der Heijden, G., Giezen, J.J. and Kramers, H.C., *Physica* 61 (1972) 566; Commun. Kamerlingh Onnes Lab., Leiden No. 394c.

## Samenvatting

In dit proefschrift worden experimenten besproken die verricht zijn aan het koeffect dat optreedt wanneer vloeibaar helium beneden de lambda temperatuur gedwongen wordt te stromen door een thermisch geïsoleerd systeem bestaande uit een superlek en een capillair welke via een kamer waarin de koeling optreedt met elkaar verbonden zijn.

In hoofdstuk I wordt het gedrag van de temperatuur van de kamer,  $T_a$ , als functie van de badtemperatuur en het voor de stroming verantwoordelijke opgelegde drukverschil over het stromingscircuit onderzocht. In hoofdstuk II worden eveneens metingen van  $T_a$  nu als functie van de druk waaronder het helium verkeert en de stroomsnelheid door het capillair beschreven. Deze experimenten werden ook verricht in de aanwezigheid van een regelbare warmtetoevoer aan de kamer. In hoofdstuk III tenslotte wordt een uitbreiding beschreven van de in hoofdstuk I behandelde experimenten, die hieruit bestaat dat nu ook het gedrag van de temperatuur langs het capillair wordt onderzocht.

Uit de experimenten beschreven in hoofdstuk I blijkt dat ongeacht welke begintemperatuur voor het experiment wordt gekozen, althans voorzover deze boven 1 K ligt, de koeling in de kamer beperkt blijft tot ongeveer 0.75 K. Er kon worden aangetoond dat deze limiet niet veroorzaakt wordt door een eventueel warmtelek over het superlek. Daarentegen wordt indien het experiment verricht wordt uitgaande van een badtemperatuur lager dan 1 K geen koeling meer waargenomen. Integendeel, in de experimenten verricht bij een badtemperatuur van 0.5 K werd een sterke opwarming waargenomen. Deze opwarming kon beschreven worden met een homogene dissipatie in het capillair en een effectieve warmtegeleidingscoëfficiënt welke blijkt overeen te stemmen met literatuurwaarden van Fairbank en Wilks.

Dit resultaat wijst erop dat bij 0.5 K er geen convectief warmtetransport is hetgeen consistent is met het feit dat geen koeling, die juist ten nauwste samenhangt met convectief warmtetransport, meer optreedt.

Voor wat betreft de metingen die bij een badtemperatuur hoger dan 1 K werden verricht kon worden aangetoond dat in geval de limiterende temperatuur nog niet is bereikt de drukval over het capillair nul is, hetgeen op grond van de bewegingsvergelijkingen impliceert dat in dat geval de wederkerige wrijvingskracht tussen superfluide en normale component het temperatuurverschil over het capillair in standhoudt. In de eerste plaats was de bedoeling van de in hoofdstuk II beschreven experimenten de in hoofdstuk I uitgesproken verwachting dat de minimumtemperatuur zal afnemen naarmate de druk waaronder het helium verkeert



hoger is te toetsen. Inderdaad wees het experiment uit dat deze verwachting juist is; bij een druk van 24.75 atmosfeer ligt het minimum ongeveer 0.1 K lager dan bij de verzadigde dampspanning. Vastgesteld werd dat de oorzaak voor het optreden van een limiettemperatuur voor koeling gelegen is in een warmte-toevoer naar de kamer. Of deze veroorzaakt wordt door dissipatie in de kamer zelf of door een (niet convectieve) toevoer van in het capillair vrijkomende warmte kon niet met zekerheid worden uitgemaakt.

Aan de hand van het gedrag van  $T_a$  als functie van de stroomsnelheid, waar- bij met behulp van de regelbare warmtetoevoer aan de kamer de normaalsnelheid in het capillair onafhankelijk kon worden gevarieerd, werd de aard van de voor de koeling zo belangrijke wederkerige wrijvingskracht nader onderzocht. Het bleek dat een wederkerige wrijvingskracht van het Gorter-Mellink type, dat wil zeggen een kracht evenredig met de derdemacht van de relatieve snelheid van normaal-en superfluidum althans voor wat betreft de hoge drukmetingen een goede fenomenologische beschrijving van het gedrag van  $T_a$  geeft. Dit geldt ook voor die experimenten waarbij de stroomrichting naar het superlek toe is en er op- warming van de kamer optreedt. De evenredigheidsconstante (de Gorter-Mellink wederkerige wrijvingsconstante  $A$ ) is bij een druk van 10 atm bepaald. Qua orde van grootte en temperatuurafhankelijkheid bleek deze overeen te stemmen met literatuurwaarden van Vinen.

De metingen van de temperatuurverdeling langs het capillair beschreven in hoofdstuk III dienen er ondermeer toe een antwoord te geven op een aantal vragen die in de twee eerste hoofdstukken naar voren kwamen. De gemeten waarde van de temperatuurgradiënt aan de ingang van het capillair bleek tesamen met de geëx- trapoleerde waarde voor de warmtegeleidingscoëfficiënt die in hoofdstuk I werd gevonden van de goede orde van grootte om warmtegeleiding vanuit het capillair naar de kamer een mogelijke oorzaak voor het optreden van de limiet te doen zijn. Dit wil echter nog niet zeggen dat dissipatie in de kamer als oorzaak uitgeslo- ten is. De temperatuurdistributie gevonden bij lage snelheden bleek niet in overeenstemming met het Gorter-Mellink model. Voor hoge snelheden wordt de temperatuurverdeling onafhankelijk van de badtemperatuur voor praktisch de gehele lengte van het capillair. Op grond van de thermodynamica wordt aangetoond dat de in het capillair gedissipeerde energie afgevoerd wordt naar het bad uit- sluitend door convectief warmtetransport, waarbij de snelheid van de normale component aan het eind van het capillair gelijk is aan de snelheid waarmee de vloeistof als geheel stroomt.

Op verzoek van de Faculteit der Wiskunde en Natuurwetenschappen volgt hier een overzicht van mijn studie.

Nadat ik in 1960 aan het St. Janscollege te 's-Gravenhage het diploma gymnasium-B behaald had, begon ik mijn studie in de natuurkunde; aanvankelijk aan de Technische Hogeschool te Delft, om vervolgens, na het afleggen van het P<sub>1</sub> examen voor natuurkundig ingenieur, deze voort te zetten aan de Rijksuniversiteit te Leiden. Het candidaatsexamen wis- en natuurkunde met bijvak sterrekunde (a<sup>1</sup>) legde ik af in april 1964, het doctoraalexamen experimentele natuurkunde in december 1967.

Inmiddels was ik sedert mei 1964 werkzaam in de helium-werkgroep onder leiding van Prof. Dr. K.W. Taconis en Dr. R. de Bruyn Ouboter. De grondbeginselen van het experimentele onderzoek aan de stroming van He II leerde ik van Dr. W.M. van Alphen, die ik assisteerde bij de metingen aan de kritische doorstroomcapaciteit van superlekken, de metingen aan de dissipatie in stromend He II en de experimenten aan persisterende stromingen. Terzelfdertijd verleende ik assistentie aan mevrouw Drs. W. Passchier-Vermeer bij oriënterende metingen betreffende de adiabatische stroming van He II - welke ik sinds begin 1966 zelfstandig voortzette - , die ten grondslag liggen aan het in dit proefschrift beschreven werk.

Vanaf september 1965 assisteerde ik op het natuurkundig practicum voor precandidaten en sinds het cursusjaar 1968 leidde ik het electrisch en electronisch practicum voor studenten in de chemie.

In oktober 1966 kwam ik in dienst van de Stichting F.O.M., aanvankelijk als wetenschappelijk assistent en sedert het doctoraalexamen als wetenschappelijk medewerker. Sinds 1 oktober 1973 ben ik als wetenschappelijk medewerker aan het Natuurkundig Laboratorium van de N.V. Philips Gloeilampenfabrieken te Eindhoven verbonden.

Velen hebben een bijdrage geleverd aan het tot stand komen van dit proefschrift. Met bijzonder veel plezier denk ik terug aan de periode augustus 1968 - juli 1970 toen in samenwerking met Dr. J.K. Hoffer de experimenten beschreven in het eerste hoofdstuk werden verricht. Bij de uitvoering van de experimenten behandeld in het tweede hoofdstuk ondervond ik veel steun aan de assistentie door Drs. W. Koops. Met genoegen denk ik terug aan de vaak langdurige discussies met Dr. H. van Beelen wiens stimulerende invloed van bijzondere betekenis is geweest voor de uiteindelijke interpretatie van de veelheid aan experimentele gegevens. Ook de discussies met de overige leden van de helium-werkgroep heb ik hooglijk gewaardeerd.

Dank ben ik ook verschuldigd aan de technische en administratieve staf van het Kamerlingh Onnes Laboratorium. De heer J.D. Sprong had altijd wel een vat vloeibaar helium voor mij klaar staan. De constructie van de gebruikte apparaten werd verzorgd door de heren E.S. Prins en J.P. Hemerik, terwijl de heren L. van As en P.J.M. Vreeburg het glastechnische gedeelte voor hun rekening namen. Nimmer deed ik tevergeefs een beroep op de heren J. Turenhout, A.J.J. Kuyt, en G. Vis, die mij met raad en daad behulpzaam waren en wier werkplaats altijd voor mij openstond. De figuren in dit proefschrift werden verzorgd door de heren W.F. Tegelaar, die ook voor de foto's zorg droeg, en J. Bij.

Tenslotte ben ik dank verschuldigd aan mevrouw A. Deelder-Kamerling, die de eerste versie van het manuscript heeft getypt, en aan mevrouw E. de Haas-Walraven, die op vaardige wijze voor de typografische vormgeving van dit proefschrift heeft zorg gedragen.

